JCB Article

Postnatal NG2 proteoglycan–expressing progenitor cells are intrinsically multipotent and generate functional neurons

Shibeshih Belachew,[1,2] Ramesh Chittajallu,[1,2] Adan A. Aguirre,[1] Xiaoqing Yuan,[2] Martha Kirby,[3] Stacie Anderson,[3] and Vittorio Gallo[1,2]

[1]Center for Neuroscience Research, Children's Research Institute, Children's National Medical Center, Washington, DC 20010
[2]Laboratory of Cellular and Synaptic Neurophysiology, National Institute of Child Health and Human Development, National Institutes of Health, Bethesda, MD 20892
[3]Gene Transfer Laboratory, Hematopoiesis Section, Flow Cytometry Core Unit, National Human Genome Research Institute, National Institutes of Health, Bethesda, MD 20892

Neurogenesis is known to persist in the adult mammalian central nervous system (CNS). The identity of the cells that generate new neurons in the postnatal CNS has become a crucial but elusive issue. Using a transgenic mouse, we show that NG2 proteoglycan–positive progenitor cells that express the 2′,3′-cyclic nucleotide 3′-phosphodiesterase gene display a multipotent phenotype in vitro and generate electrically excitable neurons, as well as astrocytes and oligodendrocytes. The fast kinetics and the high rate of multipotent fate of these NG2$^+$ progenitors in vitro reflect an intrinsic property, rather than reprogramming. We demonstrate in the hippocampus in vivo that a sizeable fraction of postnatal NG2$^+$ progenitor cells are proliferative precursors whose progeny appears to differentiate into GABAergic neurons capable of propagating action potentials and displaying functional synaptic inputs. These data show that at least a subpopulation of postnatal NG2-expressing cells are CNS multipotent precursors that may underlie adult hippocampal neurogenesis.

Introduction

The identity of postnatal central nervous system (CNS)* multipotent neural stem cells (NSCs) in vivo is a matter of intense debate. To date, a lineage continuum has not yet been established between embryonic neuroepithelial and "adult" NSCs, which emerge in restricted germinative areas during the first postnatal week (Alvarez-Buylla and Temple, 1998; Alvarez-Buylla et al., 2001). Embryonic radial glia can generate neurons (Malatesta et al., 2000; Noctor et al., 2001), and adult NSCs express molecular markers (glial fibrillary acidic protein; GFAP) and ultrastructural characteristics of astrocytes (Doetsch et al., 1999; Laywell et al., 2000). However, the use of GFAP antigenicity as a feature of postnatal NSCs is not without caveats and mostly applies to the subventricular zone (SVZ; Doetsch et al., 1999).

Similar to CNS stem cells, NG2 proteoglycan–expressing progenitor cells persist and slowly proliferate throughout the adult CNS (Ffrench-Constant and Raff, 1986; Wolswijk and Noble, 1989). During CNS development, the well-characterized anatomical distribution of NG2$^+$ progenitors (Spassky et al., 1998) overlaps with areas where totipotent NSCs reside and ongoing neurogenesis occurs (Alvarez-Buylla and Temple, 1998; Temple and Alvarez-Buylla, 1999). Cells that express the NG2 chondroitin proteoglycan represent the largest pool of postnatal proliferative progenitors

S. Belachew and R. Chittajallu contributed equally to this paper.

The online version of this article includes supplemental material.

Address correspondence to Dr. Vittorio Gallo, Center for Neuroscience Research, Children's Research Institute, Room 5345, Children's National Medical Center, 111 Michigan Ave., N.W., Washington, DC 20010-2970. Tel.: (202) 884-4996. Fax: (202) 884-4988.
E-mail: vgallo@cnmcresearch.org

S. Belachew's present address is Center for Cellular and Molecular Neurobiology, Department of Neurology, University of Liège, B-4000 Liège, Belgium.

*Abbreviations used in this paper: CNP, 2′,3′-cyclic nucleotide 3′-phosphodiesterase; CNS, central nervous system; DNQX, 6,7-dinitro-2,3-quinoxalinedione; GABA, γ-aminobutyric acid; GAD, glutamate decarboxylase; GFAP, glial fibrillary acidic protein; MAP, microtubule-associated protein; NeuN, neuronal nuclei protein; NSC, neural stem cell; OPC, oligodendrocyte progenitor cell; PCNA, proliferating cell nuclear antigen; PLP, proteolipid protein; SCM, stem cell medium; SVZ, subventricular zone; TOAD-64, turned on after division, 64 kD; TTX, tetrodotoxin.

Key words: stem cell; oligodendrocyte progenitor; differentiation; adult neurogenesis; glia

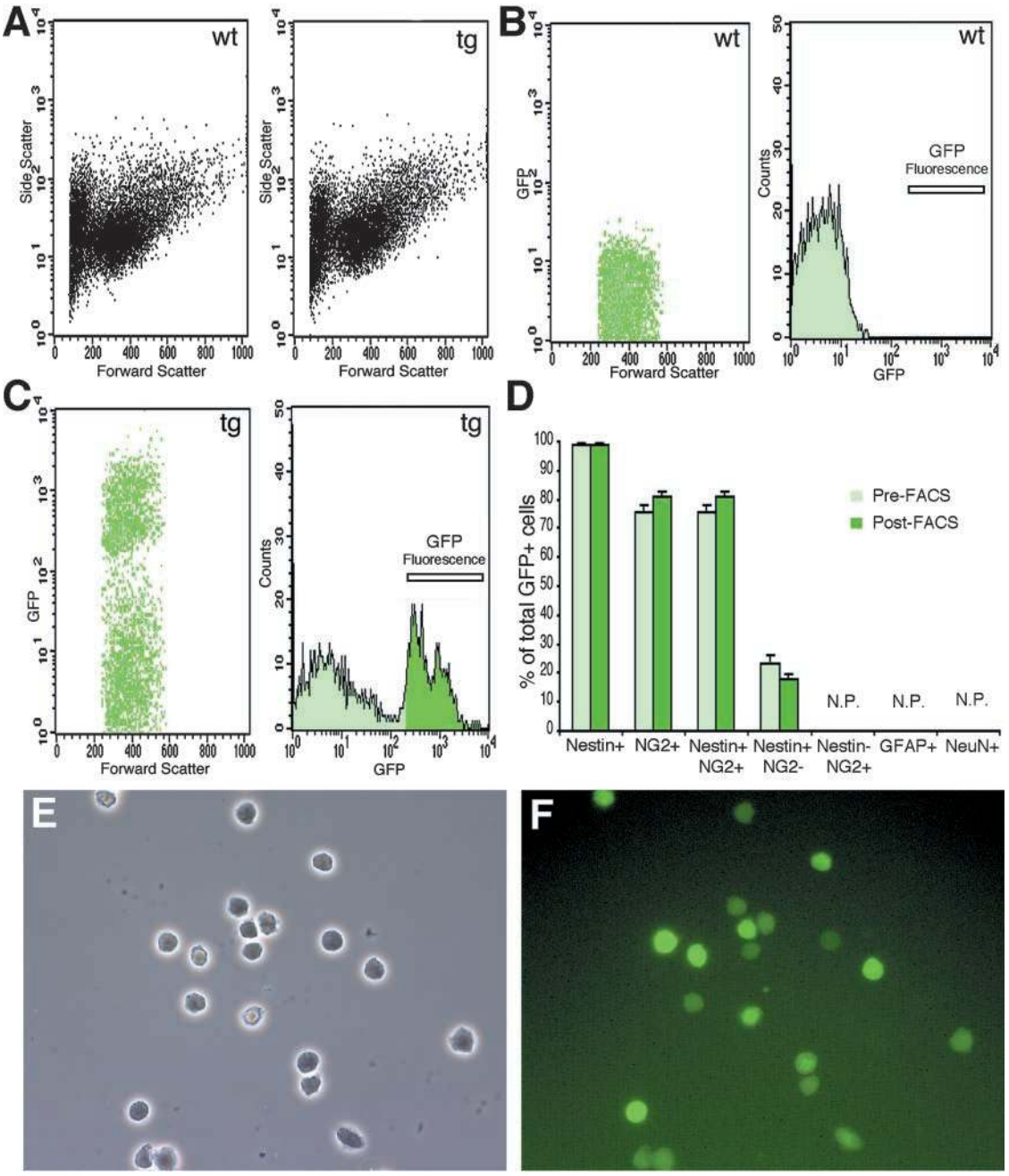

Figure 1. **FACS® purification of early postnatal GFP$^+$ cells from CNP-GFP transgenic brains reveals an NG2$^+$/nestin$^+$ phenotype.** FACS® analysis of acutely dissociated cell suspensions of P2 whole brain from CNP-GFP transgenic mice (tg) and wild-type (wt) littermates displayed identical light forward and side scatter distributions (A). To eliminate erythrocytes and cell debris, forward scatter gating parameters were chosen for further GFP fluorescence analysis (B and C, left panels). Cells from CNP-GFP suspensions that were considered GFP$^+$ and FACS®-selected, were in a range of fluorescence (C, bar in right panel) far above (ratio >5×) maximal background intensity yielded by the wild-type cell suspension (B, bar in right panel). Using such criteria, all FACS®-sorted cells were consistently found to be GFP$^+$, as determined by fluorescence microscopy analysis of cell suspensions plated on coverslips immediately after sorting, and fixed 1 h later (two independent experiments, total cells counted = 1,069, 100% were GFP$^+$; E and F). (D) Immunocytochemical characterization of pre-FACS® and post-FACS® cell suspensions (total GFP$^+$ counted cells = 1069, two independent experiments). N.P., not present. We demonstrated here that pre-FACS® versus post-FACS® GFP$^+$ cells were antigenically identical and mostly expressed an NG2$^+$/nestin$^+$ phenotype. This validated our fluorescence sorting criteria, which did not preferentially select a subset of CNP-GFP$^+$ cells. Phase-contrast (E) and fluorescence (F) views of FACS®-selected cells that were all GFP$^+$.

scattered throughout neurogenic as well as nonneurogenic areas of the CNS (Dawson et al., 2000), but their possible intrinsic stem cell potential has not yet been explored.

To determine to what extent postnatal NG2$^+$ cells may display multipotent stem cell-like properties in vitro and in vivo, we used a transgenic mouse expressing the GFP under the control of the 2′,3′-cyclic nucleotide 3′-phosphodiesterase (CNP) promoter (Belachew et al., 2001; Yuan et al., 2002). In this CNP-GFP transgenic mouse, all NG2$^+$ progenitor cells assessed in the first postnatal week were consis-

tently found to be GFP$^+$ in distinct CNP-GFP transgenic lines (Yuan et al., 2002), indicating that they also expressed the CNP gene.

In white matter regions of the CNP-GFP mice, the spatial and temporal expression pattern of GFP matched oligodendrocyte development from the progenitor stage to mature myelinating oligodendrocytes (Belachew et al., 2001; Yuan et al., 2002). Furthermore, CNP-GFP$^+$ cells expressed oligodendrocyte progenitor markers in the subventricular zone, and mature oligodendrocyte markers in the developing and adult white matter (Yuan et al., 2002). However, CNP-GFP$^+$ cells expressing the NG2 proteoglycan were also found in gray matter regions (Yuan et al., 2002).

Here, we report that acutely purified preparations of CNP-GFP–expressing cells from early postnatal brain can form clonal neurospheres in vitro. Furthermore, we demonstrate that within the CNP-GFP$^+$ population, NG2$^+$ cells represent multipotent progenitors that can rapidly generate astrocytes and mature, action potential–propagating neurons after 48 h of culture. Finally, we provide evidence that a proportion of NG2$^+$/CNP-GFP$^+$ progenitor cells may be a source of new functional neurons in the postnatal hippocampus, where neurogenesis is known to continue in adulthood.

Results

Early postnatal CNP-GFP$^+$ oligodendroglial cells form multipotent neurospheres and rapidly generate neurons, astrocytes, and oligodendrocytes in vitro

All the in vitro data were obtained from a single transgenic line (Belachew et al., 2001; Yuan et al., 2002), but were replicated in another CNP-GFP line (Fig. S2, available at http://www.jcb.org/cgi/content/full/jcb.200210110/DC1, and unpublished data). FACS® was used to generate pure GFP$^+$ cell preparations from early postnatal brain of CNP-GFP mice (Fig. 1, A–F). We characterized the nestin immunophenotype of FACS®-purified GFP$^+$ cells because nestin is an intermediate filament protein expressed in neuroepithelium-derived NSCs during development (Lendahl et al., 1990). We observed that 99.0 ± 0.6% of P2 FACS®-sorted GFP$^+$ cells were nestin$^+$. Furthermore, 81.1 ± 1.6% of FACS®-sorted GFP$^+$ cells were NG2$^+$, whereas 17.9 ± 1.6% were NG2$^-$ (Fig. 1 D; mean ± SEM, total GFP$^+$ counted cells = 1,069, two independent experiments). We also observed that only 6.24 ± 1.02% (mean ± SEM, total GFP$^+$ counted cells = 678) of acutely FACS®-purified GFP$^+$ cells expressed the CNP protein, a marker of more mature oligodendrocytes. No freshly sorted GFP$^+$ cells expressed neuronal (neuronal nuclei protein, NeuN) or astrocytic (GFAP) markers (Fig. 1 D).

To study the developmental fate of early postnatal CNP-GFP$^+$ cells, pure FACS®-sorted GFP$^+$ cells from P2 brains were cultured in stem cell medium (SCM) under two different conditions (Fig. 2 A): (1) "suspension" cultures; cells seeded on uncoated plastic to form floating clonal spheres; and (2) "adherent" monolayer cultures; cells directly plated on polyornithine-coated plastic. In suspension cultures, CNP-GFP$^+$ cells rapidly gave rise to GFP$^+$ neurospheres (Fig. 2, B and C) that displayed high levels of nestin expression (Fig. 2 D). Single clonally expanded GFP$^+$ spheres (8–10 d of suspension culture in SCM) plated on coated plastic generated both NeuN$^+$ neurons and GFAP$^+$ astrocytes in SCM (Fig. 2, E–G). Interestingly, these neurons and astrocytes derived from CNP-GFP$^+$ cells were GFP$^-$, illustrating that CNP gene expression is down-regulated when GFP$^+$ cells undergo nonoligodendroglial differentiation. Similarly, in adherent cultures, FACS®-purified CNP-GFP$^+$ cells that were nestin$^+$ and mostly NG2$^+$ (Fig. 1 D and Fig. 2, H–I) rapidly generated NeuN$^+$/GFP$^-$ neurons, GFAP$^+$/GFP$^-$ astrocytes, and mature O1$^+$/GFP$^+$ oligodendrocytes within 48 h (Fig. 2, J–L).

NG2$^+$ cells represent the multipotent cells in the CNP-GFP$^+$ lineage

To enable accurate determination of cell numbers and percentages, we restricted our quantitative analysis to adherent cultures (Fig. 2 M). We assessed cellular immunophenotypes after 48 h in SCM to prevent misinterpretation of the results due to a possible amplification of an initially undetectable contamination of our FACS®-sorted samples by GFP$^-$ cells (Fig. 1 D). The fate of total FACS®-sorted CNP-GFP$^+$ cells arising from P2 whole brain was compared with the fate of selected subpopulations of CNP-GFP$^+$ cells double-sorted according to their NG2$^+$ (Fig. 3 A) or O4$^+$ phenotype (Yuan et al., 2002).

First, we compared the fate of FACS®-sorted NG2$^+$/CNP-GFP$^+$ cells with that of total CNP-GFP$^+$ cells (Fig. 2 M). In cultures derived from purified NG2$^+$/CNP-GFP$^+$ cells, we observed: (1) a higher percentage of NeuN$^+$ neurons; (2) a lower percentage of GFAP$^+$ astrocytes; and (3) a strikingly lower percentage of nestin$^+$ cells. The different fates of NG2$^+$/CNP-GFP$^+$ cells and total CNP-GFP$^+$ cells must result from specific properties of NG2$^-$ progenitor cells that were shown to be also nestin$^+$ in the initial FACS®-purified suspensions (Fig. 1 D). Therefore, this NG2$^-$/nestin$^+$ population might account for a functionally distinct class of CNP-GFP$^+$ precursors that appears significantly less neurogenic, but more astrogliogenic than NG2$^+$/nestin$^+$ cells. The rapid down-regulation of nestin expression when FACS®-sorted NG2$^+$/nestin$^+$/CNP-GFP$^+$ cells were cultured in SCM suggests that the multipotent fate of these cells is not the result of their de-differentiation into NG2$^-$/nestin$^+$/CNP-GFP$^+$ cells.

O4$^+$/CNP-GFP$^+$ cells were also selectively FACS®-purified and cultured for 48 h in SCM. As compared with the progeny of NG2$^+$/CNP-GFP$^+$ cells, with O4$^+$/CNP-GFP$^+$ cells (Fig. 2 M) we observed (1) a significant decrease in the percentage of NeuN$^+$ neurons and GFAP$^+$ astrocytes; (2) a smaller percentage of NG2$^+$ cells; and (3) a higher proportion of O4$^+$ and O1$^+$ oligodendrocyte lineage cells. Given that the NG2 and O4 phenotypes are known to partially overlap, the fact that purified O4$^+$/CNP-GFP$^+$ cells still generated a small percentage of neurons and astrocytes was either due to the presence of NG2$^+$/O4$^+$ cells within the FACS®-selected O4$^+$/CNP-GFP$^+$ population (unpublished data), or to an intrinsic property of O4$^+$ cells. Altogether, these results suggest that a sizeable proportion of NG2$^+$ cells in culture represent postnatal multipotent precursor cells.

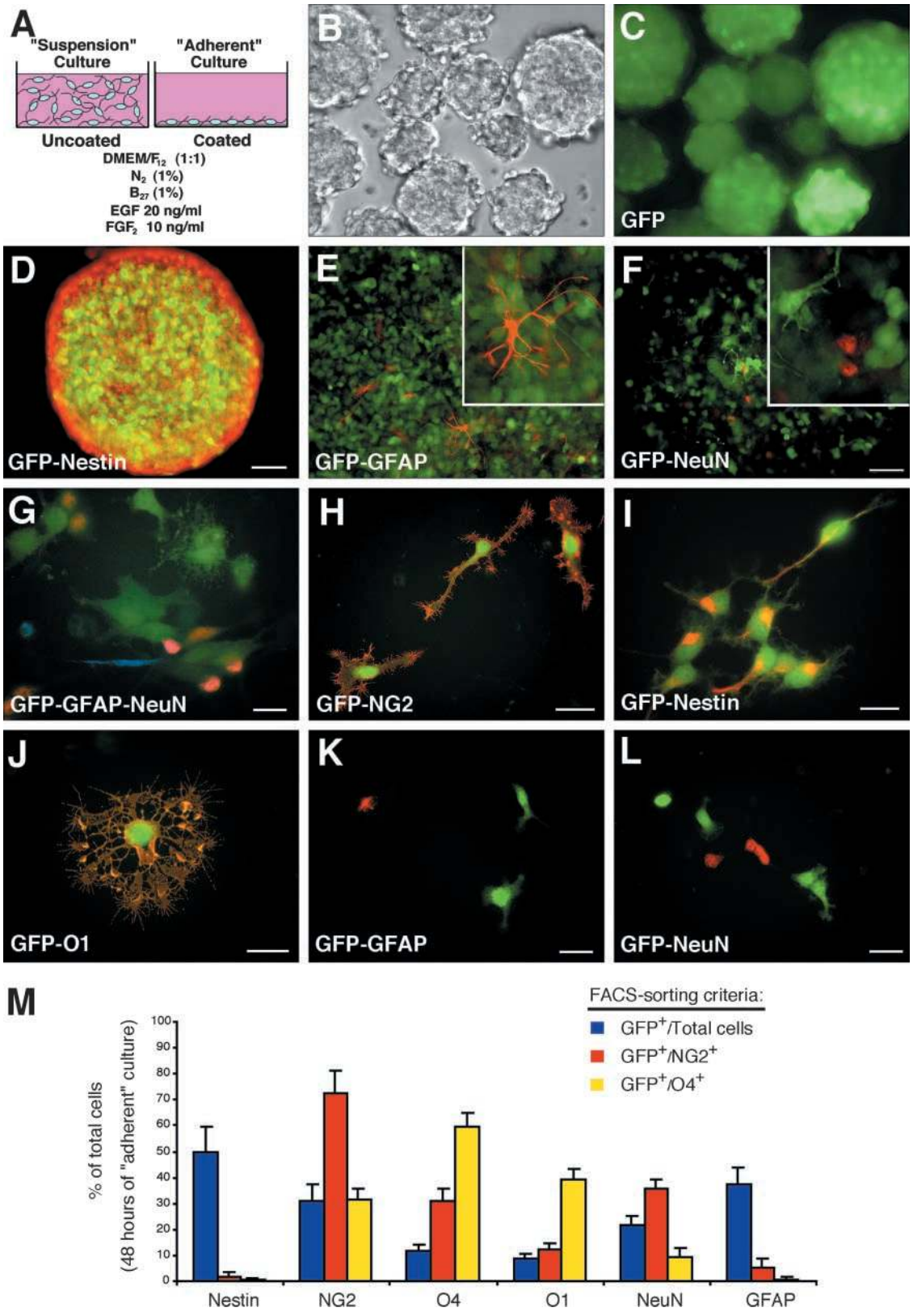

Figure 2. **Early postnatal CNP-GFP$^+$ cells generate multipotent neurospheres and give rise to neurons, astrocytes, and oligodendrocytes in vitro.** (A) Culture conditions. Phase-contrast (B) and fluorescence (C) views of GFP$^+$ neurospheres grown in suspension (5 d in vitro) on uncoated substrate in EGF- and FGF2-containing medium (SCM). (D) A clonally expanded GFP$^+$ neurosphere expressed high levels of nestin immunostaining (red). Clonal spheres gave rise to GFAP$^+$/GFP$^-$ astrocytes (E, red) and NeuN$^+$/GFP$^-$ neurons (F, red) within 2 d post-plating on polyornithine-coated coverslips. G shows GFAP$^+$ (blue) astrocytes, NeuN$^+$ (red) neurons, and GFP$^+$ oligodendroglial cells derived from a single clonal GFP$^+$ sphere. When cultured in adherent conditions, i.e., on polyornithine-coated surface directly after FACS® sorting, NG2$^+$(H, red)/nestin$^+$(I, red) GFP$^+$ cells also expressed a multipotent fate within 2 d in SCM, and generated mature O1$^+$(J, red)/GFP$^+$

Clonal analysis of cultured NG2$^+$/CNP-GFP$^+$ cells

NG2$^+$/CNP-GFP$^+$ cells were FACS®-purified (Fig. 3, A–D) and cultured at clonal dilution for 1 week in SCM. We performed two independent experiments yielding similar results, and assessed a total of 297 clones (Fig. 3 E; 18 ± 3 cells/clone, mean ± SEM, ranging from 10 to 34). The efficiency of clone generation was 0.43 ± 0.02% (number of clones/number of NG2$^+$/CNP-GFP$^+$ cells seeded). The vast majority of the clones comprised three cell types, i.e., astrocytes (GFAP$^+$), neurons (NeuN$^+$), and O4$^+$/CNP-GFP$^+$ cells (Fig. 3, E–J). No clone was found to be devoid of CNP-GFP$^+$ cells, nor to contain exclusively CNP-GFP$^+$ cells. It is noteworthy that multipotent clones obtained from clonal cultures of NG2$^+$/CNP-GFP$^+$ cells contained slightly more astrocytes than neurons (Fig. 3 F), whereas the same progenitor cells generated preferentially neurons at nonclonal dilution (Fig. 2 M).

Inverse correlation between CNP gene promoter activity and lineage progression of CNP-GFP$^+$ cells that undergo neuronal or astroglial differentiation in vitro

A gradual loss of GFP expression was observed during astroglial maturation of CNP-GFP$^+$ cells (Fig. S1). Mature astrocytes derived from CNP-GFP$^+$ cells were GFP$^-$ and displayed typical stellate shapes with intense GFAP expression in cell bodies and processes (Fig. S1, A–D). In the same cultures, we also identified GFAP$^+$ cells expressing low levels of GFP. In all these GFAP$^+$/CNP-GFP$^+$ cells, GFAP expression was restricted to their cell body (Fig. S1, E–H, arrowheads), suggesting an intermediate stage of astroglial maturation. Similarly, among NeuN$^+$ and type $2_{a,b}$ microtubule-associated protein-positive ($MAP2_{a,b}$) neurons generated from CNP-GFP$^+$ cells, we identified either cells that were totally GFP$^-$ (Fig. 4, A–D; Fig. 4 H, arrow) or cells that expressed very low levels of GFP fluorescence (Fig. 4, E–H, arrowheads).

In conclusion, neuronal or astroglial differentiation of FACS®-sorted CNP-GFP$^+$ cells is accompanied by a progressive loss of CNP gene promoter activity and a decrease in GFP expression (Fig. 4 and Fig. S1). Our data demonstrate a lineage continuum in vitro, with the existence of weakly GFP$^+$ intermediate developmental stages, between strongly CNP-GFP–expressing multipotent cells and their GFP$^-$ neuronal or astroglial progeny.

Neurons generated from NG2$^+$/CNP-GFP$^+$ cells are electrically excitable in vitro

To confirm that FACS®-sorted CNP-GFP$^+$ cells could give rise to differentiated functional neurons, we performed whole-cell patch-clamp electrophysiological experiments. To ensure their full neuronal maturation, SCM cultures of CNP-GFP$^+$ cells were switched to a pro-neuronal medium containing a combination of brain-derived neurotrophic factor and neurotrophin-3 (Vicario-Abejon et al., 2000) (Fig. 4, I–K). After 3 d under these culture conditions and consistent with a more advanced stage of neuronal differentiation, none of the NeuN$^+$ cells continued to express GFP at detectable levels (unpublished data). GFP$^-$ (Fig. 4, I and J) and GFP$^+$ (Fig. 4 K) cells were then analyzed under these conditions. Depolarization of GFP$^-$ cells by electrotonic current pulses (step size = 10–30 pA, step duration = 300 ms) elicited single or repetitive action potentials. Post-hoc immunocytochemical characterization demonstrated NeuN expression in these electrically excitable GFP$^-$ cells (Fig. 4, I and J). In contrast, all GFP$^+$ cells were NeuN$^-$ and electrically unexcitable (Fig. 4 K). Identical results were obtained from the electrophysiological analysis of neurons generated from FACS®-purified NG2$^+$/CNP-GFP$^+$ cells cultured in pro-neuronal medium. From a total of six cells recorded, all displayed action potentials on depolarization with electrotonic pulses (unpublished data).

In situ analysis of early postnatal CNP-GFP$^+$ cells reveals an NG2$^+$/nestin$^+$ proliferative phenotype

We performed an analysis of the properties of postnatal CNP-GFP$^+$ cells in situ, with a particular focus on postnatal germinative regions (i.e., SVZ and hippocampus). Consistent with our data on acutely isolated CNP-GFP$^+$ cells from the same developmental stage (Fig. 1 D), a high proportion of CNP-GFP$^+$ cells were also NG2$^+$ and nestin$^+$ at P2 in situ (Fig. 5, A–D). Direct cell counting demonstrated that 89.6 ± 1.7% (mean ± SEM, total cells counted = 483) of CNP-GFP$^+$ cells were also NG2$^+$ in the SVZ at P2, and 18.4 ± 1.6% (mean ± SEM, total cells counted = 273) of CNP-GFP$^+$ cells were NG2$^+$ in the hippocampus at P2. Because nestin immunostaining was mostly visualized in the cell processes (Fig. 5 C), we were unable to obtain an accurate quantification of the nestin phenotype in situ. Given the controversy over whether stem cells of the adult CNS are located in the ependymal or subependymal layer of lateral ventricle walls (Chiasson et al., 1999; Doetsch et al., 1999; Johansson et al., 1999; Laywell et al., 2000; Capela and Temple, 2002), it is important to point out that NG2$^+$/CNP-GFP$^+$ cells were found in the subependymal zone (i.e., SVZ) but never in the ependymal layer, from P2 to P30 (unpublished data).

Proliferation of CNP-GFP$^+$ cells in situ was investigated by studying expression of proliferating cell nuclear antigen (PCNA). As assessed by PCNA immunostaining, 67.7 ± 5.8% of CNP-GFP$^+$ cells were proliferative in P2 hippocampus (Fig. 5, E–G; mean ± SEM, n = 354 cells counted, two independent experiments). A high mitotic index of CNP-GFP$^+$ cells was also observed in the SVZ at P2, with 93.1 ± 4.1% of these cells being PCNA$^+$ (Fig. 5, H–J; mean ± SEM, n = 793 cells counted, two independent experiments).

oligodendrocytes, GFAP$^+$(K, red)/GFP$^-$ astrocytes and NeuN$^+$(L, red)/GFP$^-$ neurons. Bar: 50 μm (B–D and E–F), 25 μm (G, K, and L), and 20 μm (H–J). M shows quantitative analysis of the multipotent properties of CNP-GFP$^+$ cells. Histograms represent immunocytochemical characterization (% of total cells in y axis, immunophenotypes in x axis) of the progeny of early postnatal (P2) FACS®-purified CNP-GFP$^+$ cells cultured directly under adherent conditions for 48 h in SCM. Comparison was made between the fate of total CNP-GFP$^+$ cells (blue) versus selected subsets of CNP-GFP$^+$ cells that were FACS®-purified according to their NG2$^+$/CNP-GFP$^+$ (red) or O4$^+$/CNP-GFP$^+$ (yellow) phenotype. Nestin, NG2, O4, O1, NeuN, and GFAP phenotypes were analyzed. Values (mean ± SEM) represent averages of 2–3 independent experiments. Counting was performed separately for each staining, and the number of total cells counted (from at least 15 separate microscopic fields) ranged between 403 and 714. Significant differences reported in the Results section were all with a P value <0.001 (*t* test).

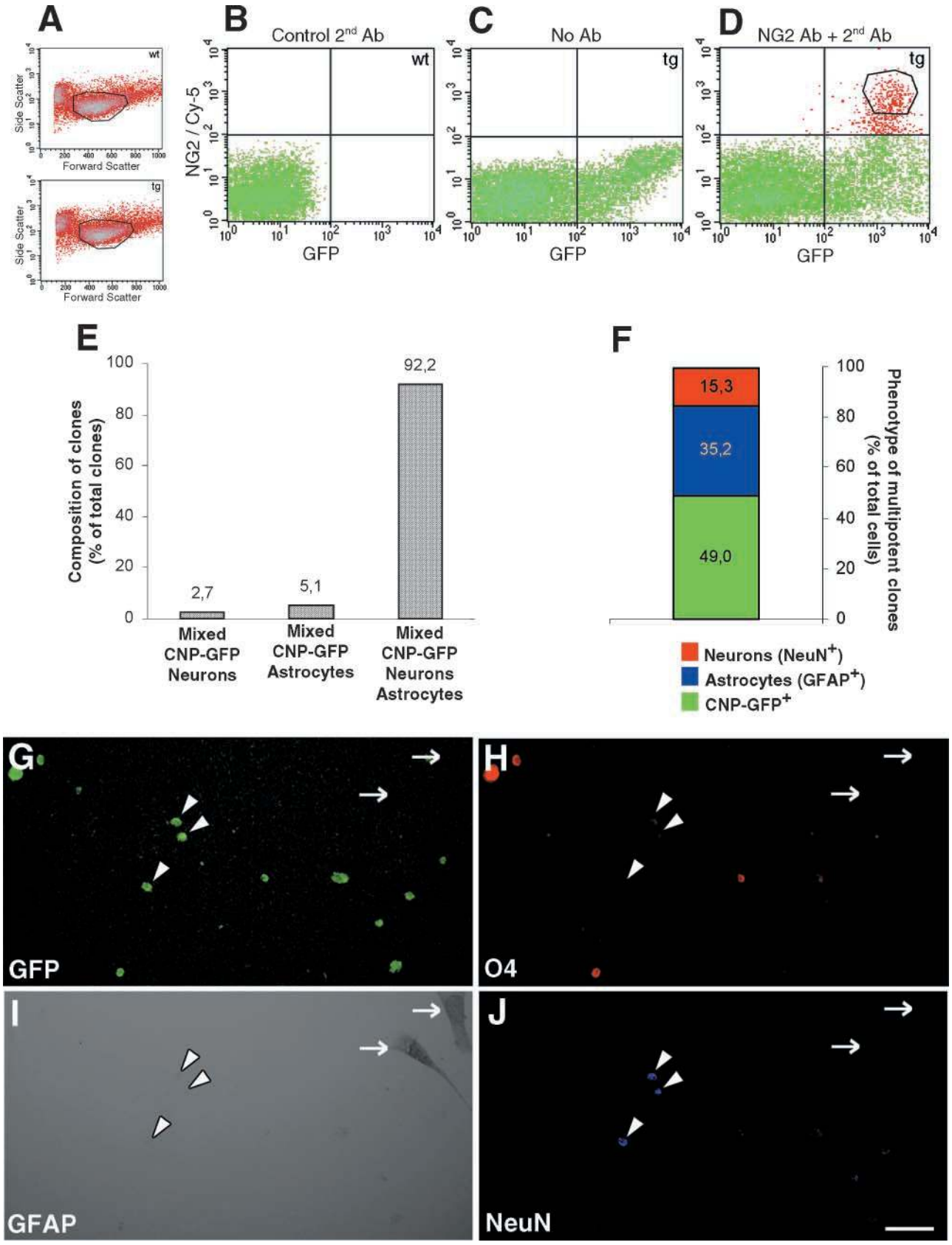

Figure 3. **Clonal analysis of NG2$^+$/CNP-GFP$^+$ cells in vitro.** (A) FACS® dot plots of acutely dissociated cells from wild-type (wt, top) and CNP-GFP transgenic brains (tg, bottom), in forward and side scatter with a polygon indicating the gate selecting the viable cells. (B–D) Sorting profiles of acutely isolated cell suspensions from P2 brains of wild-type (B) and CNP-GFP transgenic mice (C and D) dot plotted according to fluorescence intensity for GFP (x axis, logarithmic scale) and Cy-5 (fluorescence associated to secondary antibody recognizing NG2 immunoreactivity, y axis, logarithmic scale). (B) Control wild-type cells that were incubated only with the Cy-5–conjugated secondary antibody

A subset of CNP-GFP$^+$ hippocampal cells expresses neuronal markers and are electrically excitable in vivo

To determine whether highly proliferative postnatal CNP-GFP–expressing cells were also able to generate neurons or astrocytes in vivo, we investigated the existence of intermediate stages of neuronal and astroglial differentiation (i.e., expressing low levels of GFP) in CNS germinative areas. We were unable to find even a single cell expressing both GFAP and GFP between P2 and P10, either in the hippocampus or in the SVZ (unpublished data). Conversely, we found that numerous postnatal CNP-GFP$^+$ cells were also NeuN$^+$ in the hippocampus (Fig. 6, A–I). Hippocampal NeuN$^+$/CNP-GFP$^+$ committed neurons all expressed low levels of GFP (Fig. 6 J), and were mostly distributed at P6 within stratum radiatum and lucidum of CA1 and CA3 (Fig. 6, A–F; Fig. 6, C and F, arrowheads), and in the molecular layer and hilar region of the dentate gyrus. Scattered NeuN$^+$/CNP-GFP$^+$ neurons were also observed in the CA1 (unpublished data) and CA3 (Fig. 6, A–F) pyramidal layers and in the granule layer of the dentate gyrus. Postnatal NeuN$^+$/CNP-GFP$^+$ hippocampal neurons were identified in two different CNP-GFP transgenic lines (unpublished data).

NeuN$^+$/CNP-GFP$^+$ neurons were also studied by whole-cell voltage-clamp electrophysiology in P3 to P8 hippocampal slices. We recorded exclusively from CNP-GFP$^+$ cells that were selected according to their low level of GFP expression because the average GFP fluorescence intensity of NeuN$^+$/CNP-GFP$^+$ hippocampal neurons was 3.5-fold lower than NeuN$^-$/CNP-GFP$^+$ cells (Fig. 6 J; Fig. 6, G–I, arrowhead). Depolarization of such weakly CNP-GFP$^+$ hippocampal cells triggered repetitive action potentials in all of the eight cells tested (Fig. 6, K and L). Application of 1 μM tetrodotoxin (TTX) totally abolished these action potentials (five cells tested, unpublished data). Post-hoc immunostainings demonstrated that the biocytin-filled CNP-GFP$^+$ hippocampal cells that were recorded and that displayed action potentials (four cells tested) were consistently NeuN$^+$ (Fig. 6, M–O).

The anatomical and developmental distribution of NeuN$^+$/CNP-GFP$^+$ neurons in the hippocampus correlates with restriction of postnatal neurogenesis to the dentate gyrus

NeuN$^+$/CNP-GFP$^+$ cells were not only observed at early postnatal stages, but also in the adult hippocampus (P30). In all hippocampal regions, but particularly in CA1 and CA3, we observed that the absolute density of NeuN$^+$/CNP-GFP$^+$ cells and the total number of CNP-GFP$^+$ cells decreased during postnatal maturation, between P6 and P30 (Fig. 7, A and B). At P30, the density of NeuN$^+$/CNP-GFP$^+$ cells followed a clear anatomical gradient: dentate gyrus > CA3 > CA1 (Fig. 7 B). In parallel, total CNP-GFP$^+$ cells were distributed according to the same gradient (Fig. 7 B). Finally, except in CA1, the percentage of CNP-GFP$^+$ cells that expressed NeuN in the hippocampus remained constant between P6 and P30, and was maximal in the dentate gyrus (Fig. 7, C and D). These findings suggest that the intrinsic neurogenic potential of CNP-GFP$^+$ cells in CA3 and dentate gyrus may not decrease in adulthood. These results could also indicate that the decrease in the absolute number of multipotent CNP-GFP$^+$ cells might underlie the reduction of newly formed NeuN$^+$/CNP-GFP$^+$ neurons in the adult hippocampus.

A lineage continuum between NG2$^+$/CNP-GFP$^+$ progenitor cells and NeuN$^+$/CNP-GFP$^+$ neurons in the adult dentate gyrus

In the dentate gyrus of adult (P30) hippocampus, we observed that some CNP-GFP$^+$ cells also expressed TOAD-64 (turned on after division, 64 kD) protein (Fig. 8, A–H), a transient marker of early post-mitotic neurons that is expressed before most neuron-specific proteins during neurogenesis (Minturn et al., 1995a, 1995b; Cameron and McKay, 2001). TOAD-64 is also referred to as collapsin response-mediated protein 4 (Seki, 2002). In P30 dentate gyrus and CA3 areas, 11.3 ± 3.8% of CNP-GFP$^+$ cells were TOAD-64$^+$ (mean ± SEM, n = 244 total counted cells, two independent experiments). Hippocampal TOAD-64$^+$/CNP-GFP$^+$ immature neurons (Fig. 8, A–H, white arrows) reliably expressed levels of GFP fluorescence higher than NeuN$^+$/CNP-GFP$^+$-differentiated neurons (Fig. 8, A–D, arrowheads), consistent with the hypothesis that a gradual loss of CNP gene expression correlates with neuronal differentiation of CNP-GFP$^+$ cells. Moreover, the vast majority of TOAD-64$^+$/CNP-GFP$^+$ immature neurons were found to be NG2$^+$ (90%, total cells counted = 262) in the adult dentate gyrus (Fig. 8, E–H, white arrows), whereas NeuN$^+$/CNP-GFP$^+$ neurons were NG2$^-$ (Fig. 8, I–L, arrows), except for a small percentage of cells (5%; total counted cells = 754). However, in these cells, NG2 staining appeared ambiguous and suggested either a low level of NG2 proteoglycan expression or a close enwrapping of the cells within an intricate network of NG2$^+$ processes from neighboring CNP-GFP$^+$ cells (Fig. 8, I–L, arrowhead). Colocalization of TOAD-64 and NeuN expression in CNP-GFP$^+$ cells was only observed in cells displaying a weak nuclear pattern of TOAD-64 expression (Fig. 8, A–D, white arrowheads) different from the classical perinuclear distribution of this protein (Fig. 8 B, white arrows). We could also visualize TOAD-64$^+$ adult hippocam-

without anti-NG2 primary antibody. Crossed black lines in B–D represent thresholds of fluorescence. It was observed that <0.01% (limit of detection) of the control cells from B fell over this threshold. Thus, these lines determined the level of fluorescence above which cells from CNP-GFP brains (C) were selected as GFP$^+$ (lower right quadrant). When CNP-GFP cell suspensions were immunostained for NG2 (D), NG2$^+$/CNP-GFP$^+$ cells were detected in upper right quadrant. To ensure accurate purification of NG2$^+$/CNP-GFP$^+$ cells, the sort gate for these cells (D, polygon) was defined by taking an additional margin (0.2–0.3 log units) with respect to background fluorescence levels. (E) FACS®-purified early postnatal (P2) NG2$^+$/CNP-GFP$^+$ cells were cultured at clonal density for 1 wk in SCM and the phenotype of resulting cell clones was then determined. (F) Relative proportion of the different subpopulations found in the multipotent clones, i.e., containing CNP-GFP$^+$ cells, as well as neurons (NeuN$^+$) and astrocytes (GFAP$^+$). (G–J) GFP fluorescence (G, green), O4 (H, red), GFAP (I, peroxidase reaction), and NeuN (J, blue) stainings of the same microscopic field showing a representative multipotent clone derived from the growth of a single NG2$^+$/CNP-GFP$^+$ cell after one week in SCM. NeuN$^+$ cells (arrowheads) are still retaining CNP-GFP fluorescence at this stage, whereas in GFAP$^+$ astrocytes GFP expression has been lost (arrows). Bar, 50 μm for G–J.

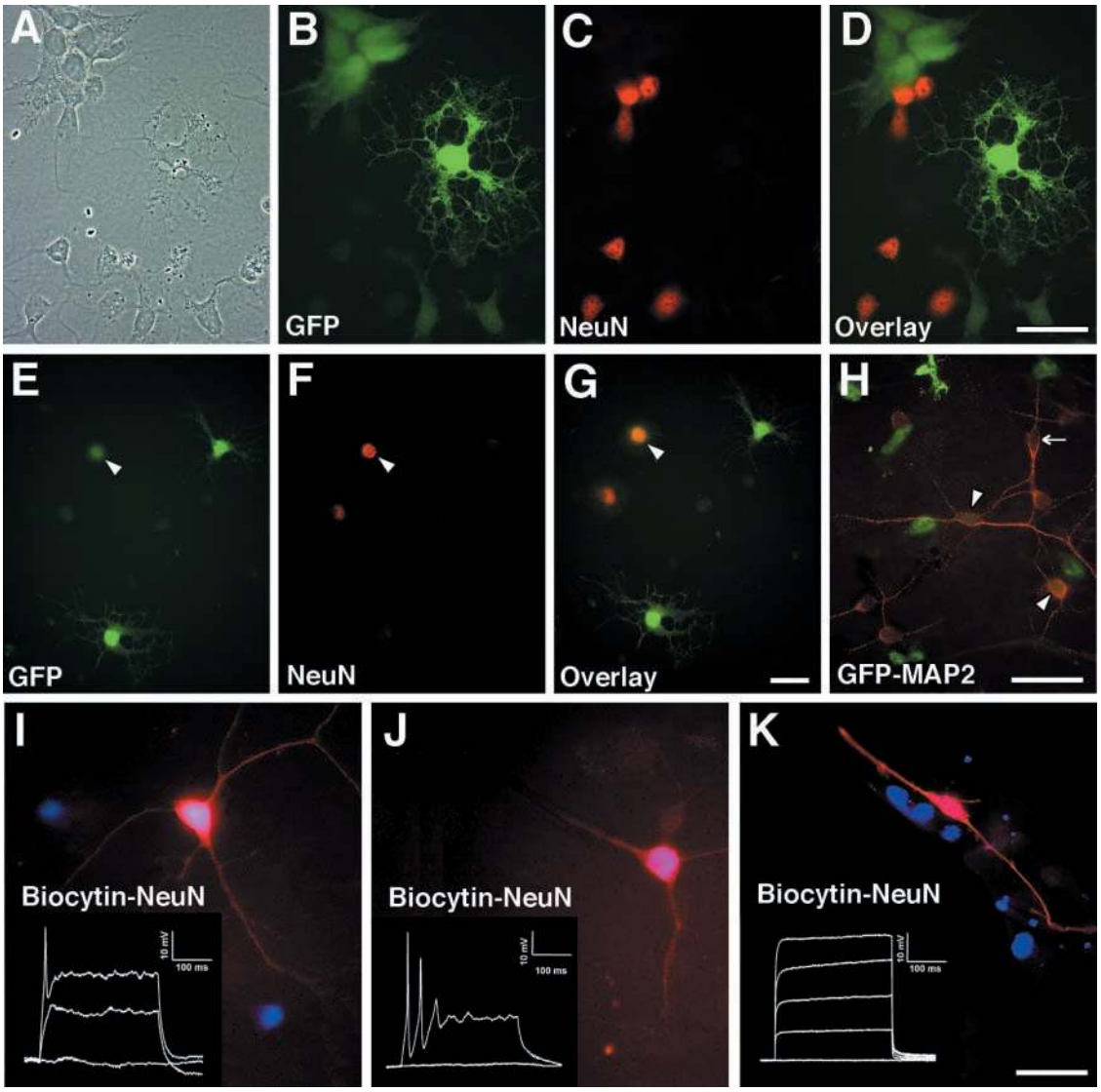

Figure 4. **CNP-GFP$^+$ cells gradually lose GFP expression as they differentiate into mature, excitable neurons in culture.** Phase-contrast view (A), GFP green fluorescence (B), NeuN staining (C, red), and overlay (D) of the same microscopic field showing NeuN$^+$/CNP-GFP$^-$ neuronal progeny derived from P2 FACS®-purified CNP-GFP$^+$ cells after 48 h in SCM. Cells expressing low levels of GFP, but displaying a neuronal phenotype could also be found (E–H). These cells expressed the neuronal markers NeuN (same microscopic field with GFP green fluorescence in E, red NeuN staining in F, and overlay in G) and MAP2$_{a,b}$ (H, red staining). Arrowheads indicate NeuN$^+$/CNP-GFP$^+$ (E–G) and MAP2$_{a,b}$$^+$/CNP-GFP$^+$ cells (H). Arrow in H points to a MAP2$_{a,b}$-expressing neuron that has completely lost GFP expression. (I–K) Electrophysiological whole-cell patch-clamp experiments in current-clamp mode were performed, in order to study excitability of cell progeny arising from SCM-cultured FACS®-sorted CNP-GFP$^+$ cells. After 2 d in SCM, cultures were switched to EGF- and FGF2-free medium supplemented with a combination of 30 ng/ml brain-derived neurotrophic factor and 30 ng/ml neurotrophin-3 for one week. GFP$^+$ and GFP$^-$ cells were analyzed and filled with biocytin during electrophysiological recording for identification and further immunocytochemical characterization. We recorded only GFP$^-$ cells that did not display a typical astrocytic morphology. Depolarization of GFP$^-$ cells elicited single (7 out of 9 cells; I, inset), or repetitive (2 out of 9 cells; J, inset) action potentials. In five of these cells, we investigated biocytin (red) and NeuN (blue) immunoreactivities, and in all cases colocalization (purple) was observed (I–J). In contrast, all GFP$^+$ cells tested (12 cells) did not elicit action potentials (K, inset). Out of the GFP$^+$ cells that were immunostained after recording (6 cells), all were NeuN$^-$ (K; biocytin in red, NeuN in blue). (I–K) GFP expression could not be visualized because of dialysis associated with whole-cell recording. Bars: 25 μm (A–D), (E–G), (H), and (I–K).

pal neurons that were CNP-GFP$^-$ (Fig. 8, A–H, red arrows) and consistently NG2$^-$ (Fig. 8, E–H, red arrows).

Adult CNP-GFP$^+$ neurons located in the hilus and inner layer of the dentate gyrus express a marker of GABAergic differentiation

To determine whether CNP-GFP$^+$ neurons found in the adult hippocampus may express phenotypic markers of functional neuronal differentiation, we performed immunohistochemical stainings for glutamate decarboxylase-67 (GAD-67), a γ-aminobutyric acid (GABA) synthesizing enzyme. In the hippocampus, GAD-67 is mostly expressed by GABAergic interneurons (Stone et al., 1999). We observed that a significant percentage of hippocampal adult CNP-GFP$^+$ cells expressed GAD-67, and all displayed low levels of GFP fluorescence (Fig. 9, A–I, arrowheads). At P30, these GAD-67$^+$/

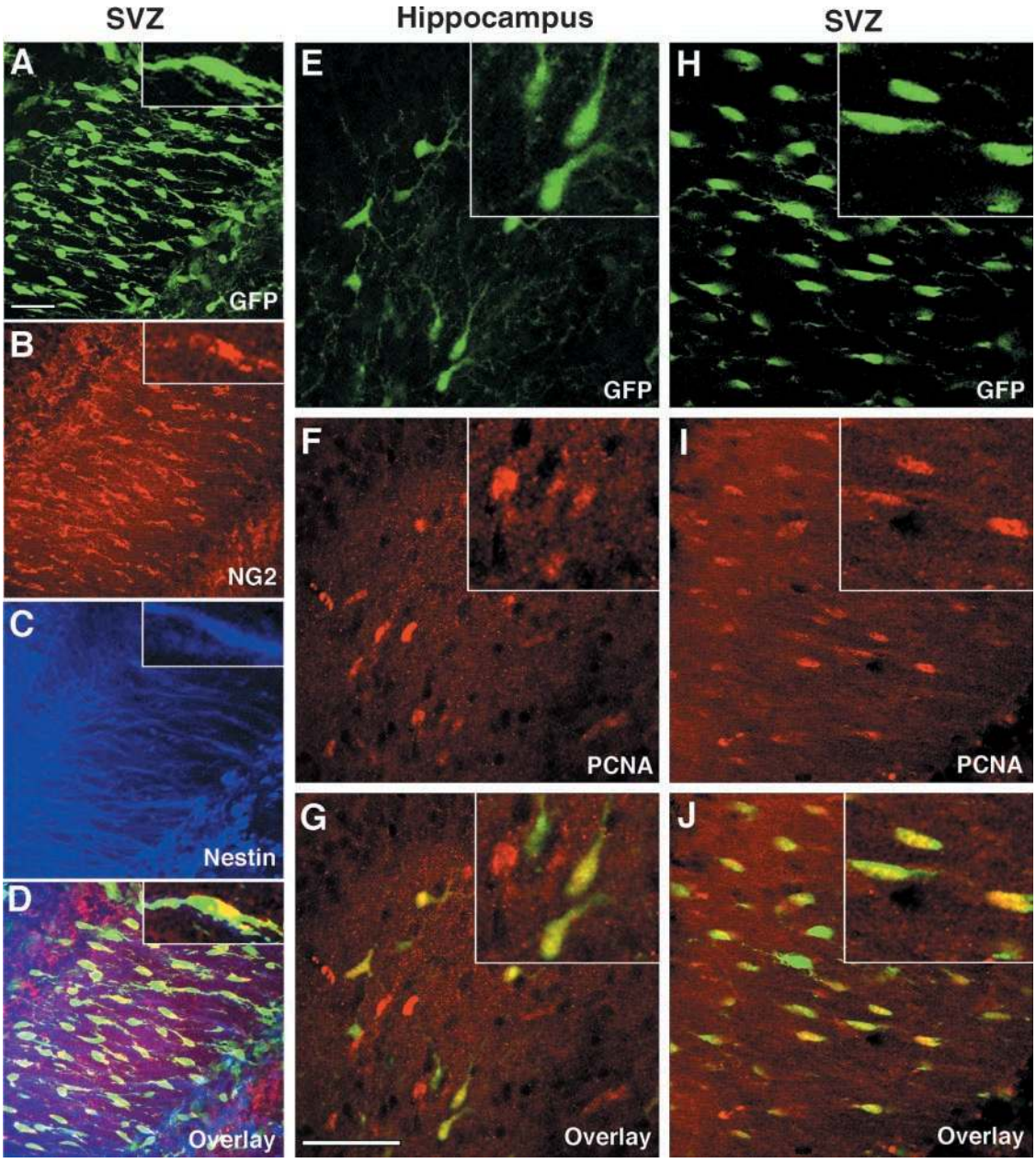

Figure 5. **Early postnatal CNP-GFP$^+$ cells are proliferative and display an NG2$^+$/nestin$^+$ phenotype in vivo in the SVZ and hippocampus.** As illustrated by Z-series (A–D, 22-μm thickness, image steps = 0.5 μm) confocal scanning images of the same field in SVZ area from P2 CNP-GFP transgenic mice, CNP-GFP$^+$ cells expressed an NG2$^+$/nestin$^+$ phenotype. 1-μm thick single plane images of a single cell at high magnification are provided in insets of A–D. The same phenotype was observed in the hippocampus (not depicted). (A) GFP green fluorescence, (B) NG2 staining, (C) nestin staining, (D) overlay. As shown in E–J (high magnification in insets), CNP-GFP$^+$ cells were proliferative in vivo. 0.5-μm thick single plane confocal scanning images of CA3 stratum radiatum area of hippocampus (E–G) and SVZ (H–J) from P2 CNP-GFP transgenic mice. (E and H) GFP green fluorescence, (F and I) PCNA staining, (G and J) overlay. A high percentage of CNP-GFP$^+$ cells were PCNA$^+$ in both germinative areas. Bars: 50 μm (A–D) and (E–J).

CNP-GFP$^+$ neurons were particularly concentrated in the inner granular zone of the dentate gyrus (Fig. 9, D–I, arrowheads), but few scattered cells were also seen in CA3 (Fig. 9, A–C, arrow and arrowheads) and CA1 areas. In the adult dentate gyrus (P30), a large proportion (~90%) of NeuN$^+$/CNP-GFP$^+$ hippocampal neurons were GAD-67$^+$, and all GAD-67$^+$/CNP-GFP$^+$ were found to be NeuN$^+$ (unpublished data). Mature neurons expressing GAD-67 and low levels of GFP were consistently CNP protein-negative (Fig. S3). Even though keeping a detectable level of transcriptional activation of the CNP gene, these GABAergic neurons have thus completely down-regulated CNP protein expression.

Postnatal hippocampal CNP-GFP$^+$ neurons receive functional synaptic inputs

To investigate whether CNP-GFP$^+$ neurons from postnatal hippocampus receive functional synaptic innervation, whole-cell voltage-clamp recordings were obtained from CNP-GFP$^+$ cells displaying low levels of GFP fluorescence in dentate gyrus (3 cells) and CA3 (14 cells) regions of P10-P12

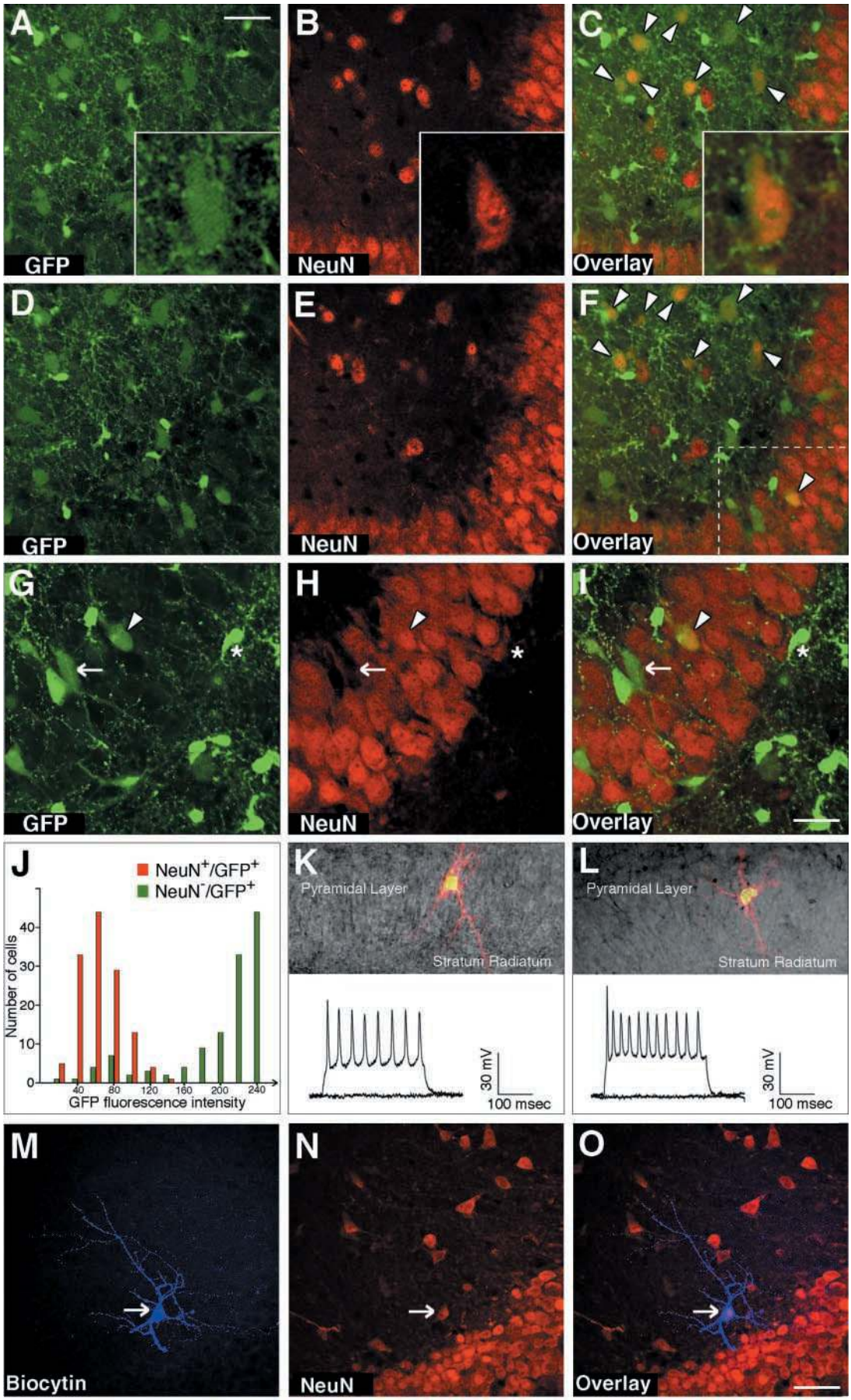
A
GFP
B
NeuN
C
Overlay
D
GFP
E
NeuN
F
Overlay
G
GFP
H
NeuN
I
Overlay
J
NeuN+/GFP+
NeuN-/GFP+
Number of cells
GFP fluorescence intensity
K
Pyramidal Layer
Stratum Radiatum
30 mV
100 msec
L
Pyramidal Layer
Stratum Radiatum
30 mV
100 msec
M
Biocytin
N
NeuN
O
Overlay

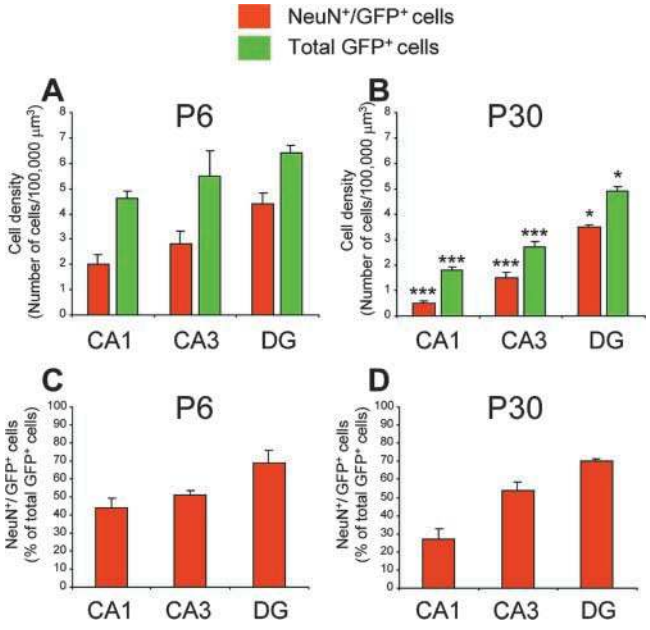

Figure 7. **Developmental and anatomical distribution of NeuN$^+$/CNP-GFP$^+$ neurons in the postnatal hippocampus.** The anatomical distribution of NeuN$^+$/CNP-GFP$^+$ cells was analyzed in Z-series confocal scanning images (20–32 μm of thickness, step size = 0.5 μm between successive images of the same field) from P6 (A and C) and P30 (B and D) hippocampus. Square fields of 228 μm^2 were separately acquired in CA1, CA3, and the dentate gyrus (DG). We calculated the absolute density of total CNP-GFP$^+$ cells and NeuN$^+$/CNP-GFP$^+$ cells in each area at P6 (A) and P30 (B). We found developmental changes in the percentage of NeuN$^+$/CNP-GFP$^+$ cells within the CNP-GFP$^+$ population only in CA1 between P6 (C) and P30 (D). Histogram values represent mean ± SEM (total GFP$^+$ cells counted = 841, two independent experiments). Statistical data pointed out in B were derived from the comparison of each P30 experimental parameter with its identical counterpart at P6. ***, $P < 0.001$; *, $P < 0.05$ (*t* test).

CNP-GFP mice. We were unable to consistently obtain recordings at older ages (i.e., P30) in these particular areas, due to the presence of brightly fluorescent neighboring cells and their associated processes (Fig. 8 and Fig. 9), which hindered reliable identification of CNP-GFP$^+$ cells expressing low levels of fluorescence. All 17 weak CNP-GFP$^+$ cells tested displayed spontaneous inward currents (Fig. 9 J). Furthermore, in seven weakly CNP-GFP$^+$ hippocampal cells, we were able to determine whether cells that exhibited spontaneous synaptic currents were also capable of eliciting action potentials on depolarization. We observed that five out of seven cells possessed both post-synaptic currents and the ability to generate action potentials. Two out of seven cells possessed synaptic currents but no action potentials, raising the hypothesis that, in the course of postnatal hippocampal neurogenesis, immature committed CNP-GFP$^+$ neuronal precursors may receive synaptic inputs first and then secondarily become capable to propagate action potentials. Importantly, we found NeuN immunoreactivity in all weakly CNP-GFP$^+$ hippocampal cells displaying synaptic currents in which we were able to perform post-hoc immunostainings (four cells; Fig. 6, M–O).

The frequency and amplitude of the spontaneous currents were clearly reduced in the presence of TTX (three cells tested), suggesting that a proportion of the spontaneous currents resulted from action potential–mediated neurotransmitter release from afferent terminals (Fig. 9 K). Furthermore, 6,7-dinitro-2,3-quinoxalinedione (DNQX; three cells tested), an antagonist of α-amino-3-hydroxy-5-methyl-4-isoxazole propionic acid and kainate subtypes of glutamate receptors, abolished all the spontaneous inward currents (Fig. 9 K). We did not expect significant activation of NMDA (*N*-methyl-D-aspartate) or chloride channel–coupled receptors such as $GABA_A$, because of the experimental conditions used (holding potential = −60 mV; calculated E_{Cl-} = −70 mV). Hence, the complete block induced by DNQX does not allow one to draw any conclusions on the existence of GABAergic inputs onto or the expression of NMDA receptors by the CNP-GFP$^+$ postnatal hippocampal neurons. Nonetheless, the finding that these postnatal CNP-GFP$^+$ neurons display spontaneous synaptic currents clearly illustrates that these cells are capable of receiving synaptic inputs in vivo.

Discussion

Using a transgenic mouse selectively expressing GFP under the influence of the CNP gene promoter, we demonstrate

Figure 6. **A subset of postnatal NeuN$^+$ hippocampal neurons express low levels of CNP-GFP and are electrically excitable.** (A–F) 0.5-μm thick single plane confocal scanning images representing two different levels (levels of planes in A–C and D–F are separated by 4 μm) of the same field of CA3 region of hippocampus from P6 CNP-GFP transgenic mice revealed that some cells were NeuN (red)-immunoreactive and expressed GFP fluorescence (A–C, insets of high magnification of a single cell). Distinct microscopic planes (A–C and D–F) within the same cells (C and F, arrowheads) showed a diffuse colocalization of the two signals, providing a more accurate demonstration of NeuN/CNP-GFP coexpression. Most of these NeuN$^+$/CNP-GFP$^+$ cells were located in the stratum radiatum, but sparse NeuN$^+$/CNP-GFP$^+$ cells were also found in the pyramidal layer (G–I, arrowhead). (G–I) Z-series (10 μm thick) confocal scanning image centered on the dashed area of (F) at higher magnification. Lower levels of GFP fluorescence were detected in all NeuN$^+$/CNP-GFP$^+$ cells (C, F, and G–I, arrowheads), as compared with CNP-GFP$^+$ cells from the same field (G–I, star), that were NeuN$^-$. Cells that expressed low levels of GFP that were NeuN$^-$ were also found (G–I, arrow). (J) Quantitative image analysis of GFP fluorescence intensity (linear arbitrary scale from 0 to 250 U; paired columns represent incremental intervals of 20 arbitrary fluorescence units) revealed a bimodal distribution, demonstrating that the average GFP fluorescence of NeuN$^+$/CNP-GFP$^+$ neurons (red) was 3.5-fold lower than that of NeuN$^-$/CNP-GFP$^+$ cells (green; total cells counted = 252, two independent experiments, equal number of cells analyzed for each population). Electrophysiological recordings were performed in weakly CNP-GFP$^+$ cells from the CA1 and CA3 pyramidal layer of P3–P8 hippocampal slices (K–L). Upper parts of K–L represent single examples of fluorescence images showing the neuron-like arborized morphology of two different CNP-GFP$^+$ cells recorded in CA3 and visualized after filling with a rhodamine-coupled dye. Lower parts of K–L display repetitive action potentials elicited by depolarizing the same cells with electrotonic current pulses (step size = 10–30 pA, step duration = 300 ms). (M–O) Representative example of a biocytin-filled (arrow in M) recorded cell in the CA3 stratum radiatum area, showing that cells that expressed low levels of GFP and that were able to propagate action potentials were consistently NeuN$^+$ (arrow in N and O) by post-hoc immunostaining. Bars: 50 μm (A–F), 33 μm (G–I), and 60 μm (M–O).

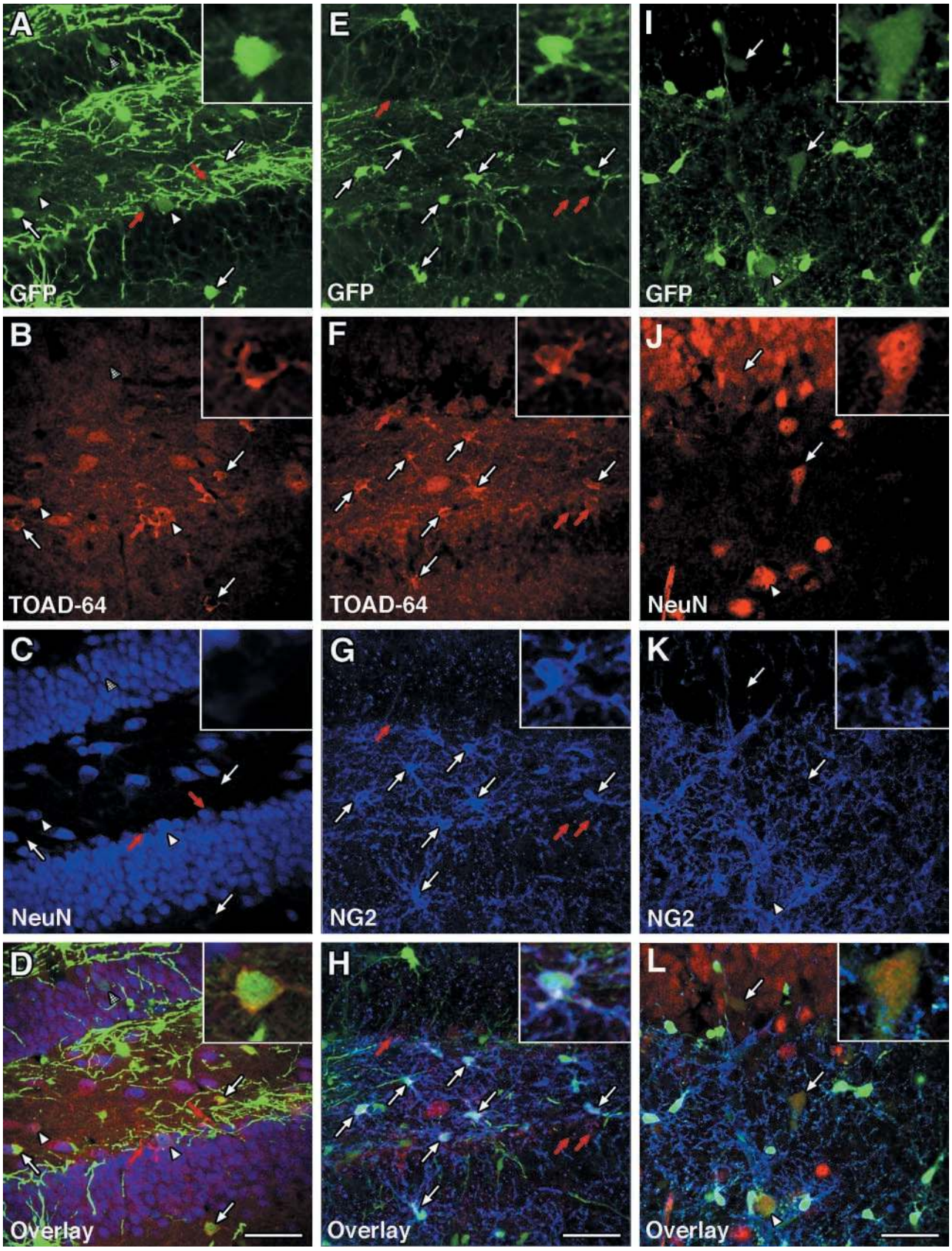

Figure 8. **The existence of NG2$^+$/TOAD-64$^+$/CNP-GFP$^+$ immature hippocampal neurons establishes a lineage continuum between NG2$^+$/CNP-GFP$^+$ progenitor cells and NG2$^-$/NeuN$^+$/CNP-GFP$^+$ neurons in the adult dentate gyrus.** Confocal photomicrographs (merged images from 4–6 optical sections of 0.5 μm each) of three representative fields of P30 hippocampal slices in which CNP-GFP$^+$ cells were immunolabeled for either TOAD-64 and NeuN (A–D, dentate gyrus), TOAD-64 and NG2 (E–H, dentate gyrus), or NeuN and NG2 (I–L, CA3). 0.5-μm thin single plane high magnification images of single cells are shown for each panel as insets located in the upper right corners (A–L). In A–D and

that postnatal NG2$^+$ progenitor cells expressing the CNP gene display antigenic and developmental features of multipotent CNS progenitor cells in vitro, including (1) a nestin$^+$ immunophenotype (Reynolds and Weiss, 1992; Johe et al., 1996); (2) the capacity to form neurospheres when cultured in uncoated conditions in EGF- and FGF2-containing medium (Reynolds and Weiss, 1992; Johe et al., 1996); and (3) the ability of a single cell to give rise to electrically excitable neurons, and to astrocytes and oligodendrocytes.

Our clonal analysis demonstrates that the multipotent fate of NG2$^+$/CNP-GFP$^+$ cells in vitro is not restricted to a minor subpopulation, but is a characteristic of a significant percentage of these progenitor cells in the early postnatal period. Moreover, because the multipotent properties of NG2$^+$/CNP-GFP$^+$ cells were reproduced in two different transgenic mouse lines, our results reflect biological properties of cells expressing the CNP gene, independent of genetic influences associated with the transgene insertion site.

To date, NG2 proteoglycan expression is the most widely used marker of postnatal progenitors in vivo (Levine et al., 2001). The mostly NG2$^+$ immunophenotype of acutely purified CNP-GFP$^+$ cells, and the quantitative comparison of the differential fate of NG2$^+$/CNP-GFP$^+$ and O4$^+$/CNP-GFP$^+$ cells versus total CNP-GFP$^+$ cells indicate that NG2$^+$ cells, which are preferentially neurogenic in SCM, represent a significant source of multipotentiality among progenitor cells expressing the CNP gene during the early postnatal period. In a previous work, optic nerve oligodendrocyte progenitor cells (OPCs) were shown to undergo nonoligodendroglial differentiation in vitro, although this occurred through a process that required a 2-mo "reprogramming" by sequential treatments with platelet-derived growth factor, FBS, and FGF2 (Kondo and Raff, 2000). Here, we demonstrate that multipotentiality in vitro is an intrinsic feature of a sizeable subpopulation of the previously so-called NG2$^+$ OPCs. This property is readily and rapidly (48 h) displayed by NG2$^+$ progenitor cells under conditions previously shown to support stem cell growth. These results emphasize that postnatal progenitor cells expressing NG2 chondroitin proteoglycan can no longer be considered as progenitor cells restricted to an oligodendroglial fate (Dawson et al., 2000). Importantly, results obtained from O4$^+$ progenitors derived from subcortical white matter in the adult forebrain show that these cells can generate neurons in response to FGF-2 (Mason, J.L., and J.E. Goldman, personal communication; and unpublished data). Such findings indicate that in the adult brain, the neurogenic potential is maintained also in cells labeled by a marker that identifies more mature stages of the oligodendrocyte lineage. This would be consistent with previous works showing that exposure of mature oligodendrocytes to FGF-2 resulted in the down-regulation of CNP, MBP, and proteolipid protein (PLP) levels and allowed re-entrance into the cell cycle (Bansal and Pfeiffer, 1997a,b).

Consistent with our in vitro studies on acutely FACS®-purified CNP-GFP$^+$ cells, early postnatal CNP-GFP$^+$ cells from SVZ and hippocampal germinative areas appeared to be NG2$^+$/nestin$^+$, and displayed a highly proliferative phenotype in situ. We demonstrate, in the postnatal hippocampus and particularly in the dentate gyrus at the adult stage, that a subset of CNP-GFP$^+$ cells, namely NG2$^+$, can express the antigenic phenotype of differentiated neurons. Furthermore, these CNP-GFP$^+$ cells were identified as neurons not only by their expression of specific neuronal proteins, but also by their capability of eliciting action potentials in situ. We also show that the anatomical distribution of NeuN$^+$/CNP-GFP$^+$ hippocampal neurons is developmentally regulated and strikingly correlates with the well-established restricted pattern of adult hippocampal neurogenesis in the dentate gyrus (Altman and Das, 1965; Kaplan and Hinds, 1977; Kuhn et al., 1996; Gage, 2000).

In the adult brain, we observed that early post-mitotic CNP-GFP$^+$ immature hippocampal neurons expressing TOAD-64 (Cameron and McKay, 2001) were also NG2$^+$ and displayed high levels of GFP, whereas more differentiated NeuN$^+$/CNP-GFP$^+$ neurons were NG2$^-$ and all exhibited low levels of GFP fluorescence. This finding indicates that NG2 proteoglycan expression and CNP gene promoter activity, as assessed by GFP fluorescence intensity, are inversely correlated with the progression of neuronal differentiation in vivo. These results are consistent with our in vitro data showing that the lineage continuum between NG2$^+$ cells and their neuronal and astroglial progeny encompassed intermediate stages of commitment, which displayed low levels of GFP expression and the differentiated neural cell markers GFAP or NeuN. Hence, altogether these results delineate a possible developmental link between a defined class of adult progenitor cells expressing NG2 chondroitin proteoglycan and the CNP gene, and newborn postnatal hippocampal neurons (Fig. 10). Although we cannot assess with the present model to what extent NG2$^+$/CNP-GFP$^+$ postnatal progenitor cells may totally repress CNP gene transcription during terminal stages of neuronal differentiation in vivo, we propose the following developmental scheme of postnatal/adult neurogenesis from NG2$^+$/CNP-GFP$^+$ cells in the hippocampus: NG2$^+$/CNP-GFP^{+++} $\rightarrow$ TOAD-64$^+$/NG2$^+$/CNP-GFP^{2+} $\rightarrow$ NeuN$^+$/NG2$^-$/CNP-GFP$^+$ $\rightarrow$ NeuN$^+$/NG2$^-$/CNP-GFP$^-$ (Fig. 10).

Using similar GFP fluorescence criteria for tracking their fate, we found no evidence that CNP-GFP$^+$ cells could generate GFAP$^+$ astrocytes in the noninjured postnatal brain. However, this discrepancy between in vitro and in vivo could be due to full repression of CNP-GFP expression in astrocytes in vivo before GFAP expression.

To place our results in the context of other works indicating that a subset of GFAP$^+$ astrocytes can generate newly formed adult hippocampal neurons (Seri et al., 2001) and/or stimulate adult neurogenesis by instructing hippocampal stem cells to adopt a neuronal fate (Song et al., 2002a, 2002b), we would like to emphasize the existence of TOAD-64$^+$/NG2$^-$/CNP-GFP$^-$ immature neurons in the adult dentate gyrus of CNP-GFP mice. The presence of

E–H, white arrows point to NG2$^+$/TOAD-64$^+$/CNP-GFP$^+$ early post-mitotic neurons that expressed levels of GFP higher than differentiated NG2$^-$/NeuN$^+$/CNP-GFP$^+$ neurons (A–D, arrowheads; I–L, arrows). Red arrows in A–D and E–H depict TOAD-64$^+$ neuronal cells that did not express CNP-GFP. Bars, 50 μm for all panels.

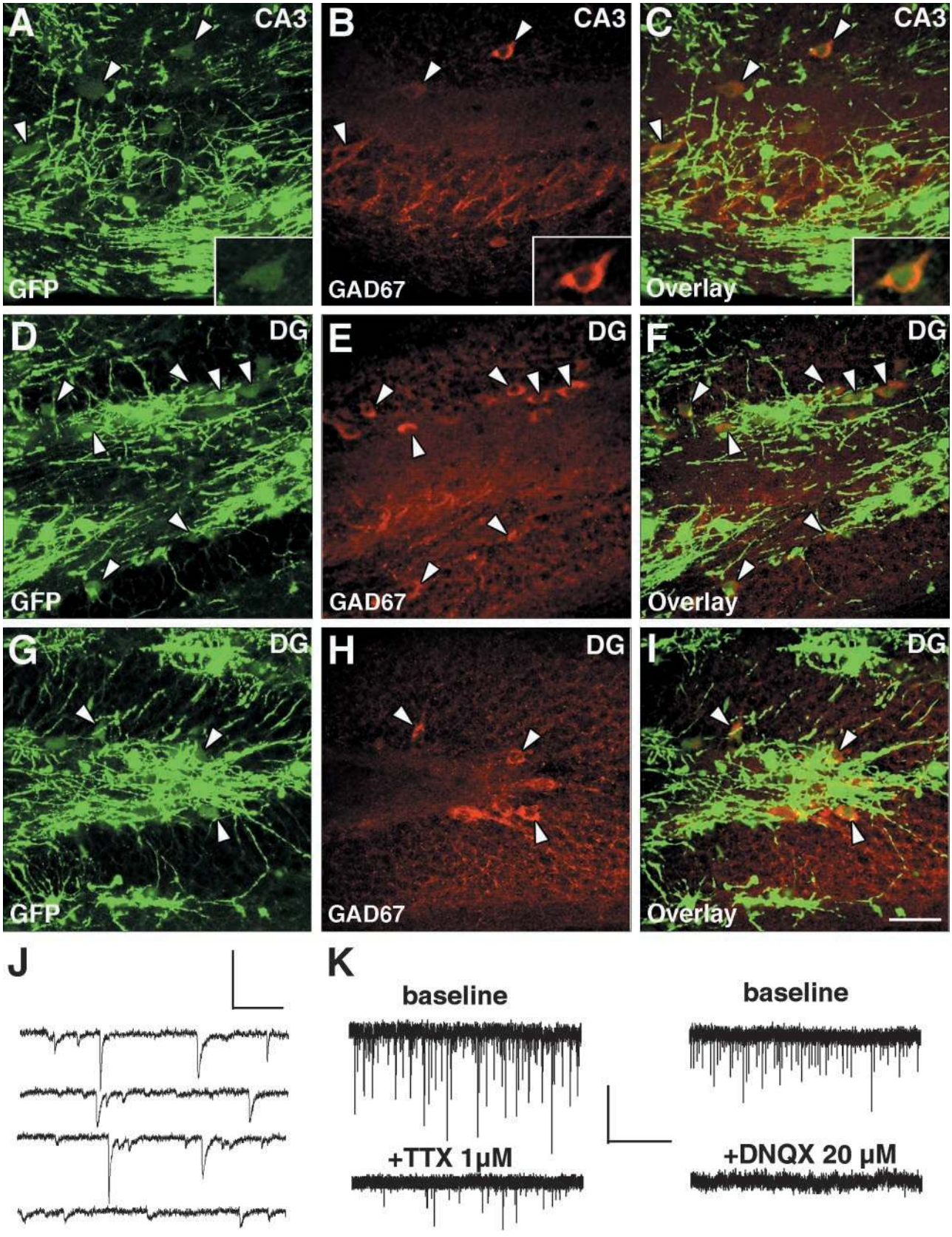

Figure 9. **CNP-GFP$^+$ postnatal hippocampal neurons are mostly GABAergic and receive functional synaptic inputs.** Representative confocal images from CA3 (A–C) and dentate gyrus (D–F and G–I; merged images of 4–6 optical sections of 0.5–0.75 μm); three adjacent fields of the same P30 hippocampal slice showed the typical spatial distribution of CNP-GFP$^+$ cells immunoreactive for GAD-67 (examples depicted by arrowheads). 0.5-μm thin single plane high magnification images of a single cell are shown in A–C as insets located in the lower right corners. All GAD-67$^+$/CNP-GFP$^+$ neurons displayed relatively low levels of GFP fluorescence. Bar, 50 μm for all panels A–I. (J) Continuous recording

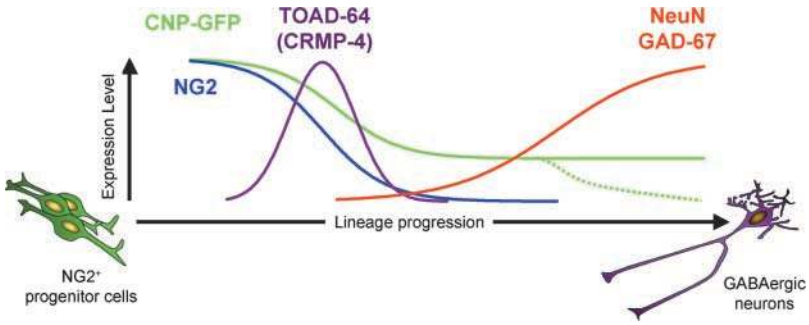

Figure 10. **Developmental regulation of neural markers in CNP-GFP lineage cells.** This scheme represents a summary of the antigenic markers expressed at different stages of neuronal differentiation of NG2+/CNP-GFP+ cells in the postnatal hippocampus.

these cells raises the issue that multiple progenitor phenotypes likely coexist to fully account for adult hippocampal neurogenesis. Rather than from another class of neuronal hippocampal progenitors, immature TOAD-64+/NG2−/CNP-GFP− cells could also directly derive from NG2+/CNP-GFP+ cells, and reflect the existence of a different pathway of neurogenesis exhibiting distinct regulation of CNP promoter activity.

In parallel with our work, a transgenic mouse expressing GFP driven by the mouse myelin (PLP) gene promoter was developed to investigate oligodendroglial lineage cells in vivo (Mallon et al., 2002). In these PLP-GFP mice, two subpopulations of NG2+ cells have been identified, based on PLP promoter (pPLP)-driven GFP expression (Mallon et al., 2002). The PLP gene is transcriptionally active in one subpopulation of NG2+ progenitors (pPLP+), which have the potential to generate mature myelinating oligodendrocytes (Mallon et al., 2002), whereas NG2+ cells that lack pPLP activity (pPLP−) could be involved in different functions. To date, there is no evidence from other reports that pPLP+ or pPLP− progenitors may undergo nonoligodendroglial differentiation (Fuss et al., 2000; Mallon et al., 2002). Our previous data provided evidence that in the CNP-GFP mice, GFP expression in white matter regions is sustained in the entire oligodendroglial lineage throughout development (Yuan et al., 2002). Furthermore, the entire postnatal NG2+ population, including both pPLP+ and pPLP− OPCs, displays high levels of GFP expression (Yuan et al., 2002). Therefore, we cannot yet distinguish whether the multipotent properties of NG2+/CNP-GFP+ postnatal progenitor cells are related to differences between the pPLP+ and pPLP− subpopulations.

Recently, it has been shown that newly generated cells in the adult mouse hippocampus display a neuronal morphology, and possess action potentials and functional synaptic inputs similar to those found in mature dentate granule neurons (van Praag et al., 2002). It has also been shown in vitro that the progeny of adult rat NSCs, when cocultured with primary neurons and astrocytes from neonatal hippocampus, develop into electrically active neurons and integrate into neuronal networks with functional synaptic transmission (Song et al., 2002b). Consistent with these findings, our data show that postnatal hippocampal CNP-GFP+ neurons located in the dentate gyrus express both NeuN and GAD-67, and display spontaneous TTX- and DNQX-sensitive post-synaptic currents, confirming that they receive functional synaptic inputs. Recent data have demonstrated that, besides excitatory granule neurons, also functional inhibitory GABAergic neurons (i.e., basket cells) are newly generated in the dentate gyrus of adult rats (Liu et al., 2003). Therefore, we suggest that NG2+/CNP-GFP+ cells represent a sizeable pool of progenitor cells that generate new functional GABAergic neurons in the adult murine hippocampus. It remains to be investigated whether postnatal NG2+/CNP-GFP+ cells express Lewis X antigen as adult murine SVZ stem cells do (Capela and Temple, 2002), and whether they are ontogenically linked to the embryonic mouse basal forebrain multipotent stem cells that generate both GABAergic neurons and oligodendrocytes during development (He et al., 2001; Yung et al., 2002).

It is still unclear to what extent our present findings can be related to the presence of α-amino-3-hydroxy-5-methyl-4-isoxazole propionic acid receptor-mediated synaptic inputs onto adult hippocampal NG2+ cells that do not display action potentials (Bergles et al., 2000). Given the neurogenic potential of postnatal NG2+ hippocampal cells and the existence of TOAD-64+/NG2+/CNP-GFP+ neuronal progenitors in the hippocampus, one could hypothesize that the results of Bergles and colleagues were obtained from NG2+ cells committed to a neuronal fate. However, these NG2+ cells analyzed electrophysiologically (Bergles et al., 2000) were located outside of neurogenic areas (i.e., CA1), where adult NG2+ hippocampal cells may be instead restricted to an oligodendroglial fate and receive, as described, synaptic inputs from CA3 pyramidal cells.

In conclusion, our data strongly support the novel hypothesis that NG2+ cells are a source of newly-generated functional neurons in the postnatal mouse hippocampus in vivo. These findings shed new light on our understanding of the function of proliferative NG2+ cells scattered throughout the entire postnatal CNS. The lack of specific immunohistochemical markers has represented a crucial hindrance for the analysis of NSCs in the adult brain. The characterization of a defined postnatal multipotent cell phenotype will help unravel the functional heterogeneity of specific subsets of newly born neurons in the postnatal hippocampus. Multipotent NG2+/CNP-GFP+ endogenous progenitor cells

(total = 2.4 s) of spontaneous post-synaptic currents under voltage clamp (−60 mV) in a CNP-GFP+ neuron of the hilar dentate gyrus area (Scale: 0.5 s, 50 pA). (K) Synaptic activity of dentate gyrus CNP-GFP+ neurons was blocked by application of 1 μM TTX and 20 μM DNQX (Scale: 30 s, 50 pA). Spontaneous synaptic currents recorded in baseline conditions were compared with those of the same cell (bottom traces) 2 min after drug application.

may thus be considered as a major cellular target for strategies aimed at recruiting CNS postnatal repair not only in demyelinating disorders, but in a broader array of neurodegenerative diseases.

Materials and methods

CNP-GFP transgenic mouse model

As previously described by Yuan et al. (2002), the CNP-GFP transgenic mouse was generated using the 3.7-kb XbaI-HindIII sequence that contains the type I and II promoter core elements of the mouse CNP gene (Gravel et al., 1998). This fragment was ligated upstream of a 1-kb SmaI-XhoI fragment encompassing the coding sequence of the EGFP gene (Cat. No. 6064–1; CLONTECH Laboratories, Inc.; Belachew et al., 2001; Yuan et al., 2002). Transgenic line C1 (FVB/NxCB6 background) was used for all the data presented in this paper. However, it is noteworthy to point out that we were able to obtain the same results in vitro and in vivo with a distinct CNP-GFP transgenic line, A2 (Fig. S2). All animal procedures were performed according to National Institutes of Health (NIH) guidelines.

Isolation of CNP-GFP$^+$ progenitor cells by FACS® and cell culture

Brains were dissected out from P2 CNP-GFP pups and wild-type litter mates. Brain tissues were dissociated as described previously (Yuan et al., 2002) to obtain final cell suspensions resuspended in N1 + 10% FBS at a density of 10^7 cells/ml for subsequent FACS® sorting. Pre-FACS® cells were plated onto 0.1 mg/ml polyornithine-coated 25-mm coverslips and incubated at 37°C for 1 h to allow attachment before further immunocytochemical characterization.

Cells were analyzed for light forward and side scatter using a FACSVantage™ SE instrument (Becton Dickinson). Cells from the negative littermates were used to set the background fluorescence, and a size threshold was used to gate out erythrocytes and cellular debris. For double NG2/EGFP and O4/EGFP FACS® analysis, cell suspensions were initially incubated with appropriate primary antibodies (see Immunocytochemistry) and then with Cy-5–conjugated secondary antibodies (1:200; Jackson ImmunoResearch Laboratories) before any sorting. Given that NG2 chondroitin sulfate can be easily cleaved off after protease treatment (Stallcup and Beasley, 1987), we compared the percentage of NG2$^+$ cells that were detected after immunostaining with cell suspensions from P4 CNP-GFP brains dissociated with and without papain treatment, respectively. We did not observe any significant differences between these two conditions. Without protease treatment during the dissociation procedure, the percentage of NG2$^+$ cells was 97.1 ± 2% (mean ± SEM; total cells counted = 520) of what it was in the presence of protease.

After FACS®, cells were rinsed twice with PBS solution and resuspended in stem cell-like medium, i.e., DME/F12 (1:1, vol/vol) supplemented with 1% N_2, 1% B_{27} (GIBCO BRL/Life Technologies), 20 ng/ml EGF, and 10 ng/ml FGF2 (Upstate Biotechnology). For adherent cultures, FACS®-sorted cells were plated onto 0.1 mg/ml polyornithine-coated 12-mm coverslips at a density of 20,000 cells/coverslip. Cells were cultured in SCM at 37°C/10% CO_2 for 48 h with renewal of growth factors every 24 h. For suspension cultures, FACS®-sorted cells were seeded onto uncoated 24-well plates (5×10^4 cells/well) and grown in SCM with daily addition of growth factors at the concentrations listed above.

Clonal analysis

For clonal expansion of single cell–derived neurospheres, the same isolation procedure was used, but FACS®-sorted CNP-GFP$^+$ cells were initially seeded in suspension conditions at a clonal density (5 cells/μl). Immediately after their formation (2–3 d in vitro), single clonal spheres were transferred (by pipetting) into separate wells to prevent formation of aggregates.

For clonal analysis, FACS®-purified NG2$^+$/CNP-GFP$^+$ cells were seeded onto polyornithine-coated coverslips at clonal density and cultured in SCM for 1 wk with daily addition of EGF and FGF2. At this density, we never observed clonal superimpositions. The average number of clones detected per coverslip was 6.06 ± 0.2 (n = 49 coverslips; mean ± SEM). The possibility of occurrence of rare cell duplets during the initial seeding of clonal cultures would not explain the high incidence of multipotent clones obtained in SCM (Fig. 3).

Immunohistochemistry

Mice at P2, P6, P10, or P30 were anesthetized by inhalation of Forane® (Ohmeda PPD Inc.), and perfused intracardiacly with 1× PBS, followed by 4% PFA. Brains were dissected out and postfixed with 4% PFA at 4°C overnight, then transferred into a solution of 4% PFA and 10% glycerol in 1× PBS for an overnight incubation at 4°C. Fixed brains were preserved in 20% glycerol in 1× PBS.

Frozen 50-μm tissue sections were prepared as described previously (Yuan et al., 2002). Sections were incubated at RT for at least 1 h in blocking solution (1% BSA, 0.3% Triton X-100, and 20% normal goat serum in 1× PBS). Primary antibodies were diluted using carrier solution (1% BSA and 0.3% Triton X-100 in 1× PBS). Primary antibody dilutions were 1:500 for rabbit polyclonal anti-NG2 antibody (a gift from Dr. Joel M. Levine, State University of New York at Stony Brook, Stony Brook, NY), 1:1,000 for mouse monoclonal anti-PCNA (Sigma-Aldrich), 1:1,000 for mouse monoclonal anti-nestin (CHEMICON International), 1:500 for mouse monoclonal anti-NeuN (CHEMICON International), 1:1,000 for rabbit polyclonal anti-GAD-67 (CHEMICON International), 1:1,000 for mouse monoclonal anti-CNP (Sternberger Monoclonals, Inc.) and 1:1,000 for rabbit anti-TOAD-64 (CHEMICON International). Brain sections were incubated in primary antibodies at 4°C overnight. Rinse was performed in carrier solution at RT, with three changes of solution every 5–15 min. All secondary antibodies (Jackson ImmunoResearch Laboratories) were diluted 1:200 in carrier solution. Cy-5– or AMCA- or TRITC-conjugated goat anti–mouse IgGs were used for monoclonal antibodies. Cy-5– or TRITC-conjugated goat anti–rabbit IgGs were used for NG2 staining. Incubation was performed at RT for 1 h, followed by three washes as described above. Sections were then transferred into 1× PBS, mounted with Mowiol, and later imaged using a fluorescence microscope (Nikon) equipped with a laser confocal scanning system (MRC1024; Bio-Rad Laboratories).

Immunocytochemistry

NG2, O4, O1, and BrdU immunostainings were performed as described previously (Yuan et al., 1998, 2002). For other stainings, coverslips were fixed with 4% PFA in 1× PBS at RT for 10 min, then permeabilized using 0.2% Triton X-100 at RT for 10 min. Blockage was performed using blocking solution at RT for 1 h. Mouse monoclonal anti-nestin antibodies (1:1000; CHEMICON International), anti-GFAP (1:500; CHEMICON International), anti-NeuN (1:250; CHEMICON International) and anti-isoforms $2_{a,b}$ of MAP$2_{a,b}$ (1:500; Clone AP-20, Lab Vision Corp.) were diluted in carrier solution, and cells were incubated at 4°C for 1 h. Cells were then washed as described ini the Immunohistochemistry section, and incubated in AMCA- or TRITC-conjugated goat anti–mouse IgG (1:200) at 4°C for 30 min. After three washes, coverslips were rinsed in 1× PBS and mounted with Mowiol.

Electrophysiology

For electrophysiological recordings in cultures derived from FACS®-purified CNP-GFP$^+$, cells were first maintained for 2 d in SCM and then shifted to EGF- and FGF2-free DME/F12 (1:1, vol/vol) medium supplemented with 10% FBS, 1% N2, and a combination of 30 ng/ml brain-derived neurotrophic factor and 30 ng/ml neurotrophin-3. Between 3 and 6 d after culturing in this neurotrophic medium, the coverslips were transferred to a recording chamber and perfused with extracellular solution (see Online supplemental material).

Patch electrodes had resistances between 4 and 7 MΩ when filled with intracellular solution of the following composition (mM): K-gluconate 130; NaCl 10; Mg-ATP 2; Na-GTP 0.3, Hepes 10; EGTA 0.6, biocytin 5 mg/ml, adjusted to pH 7.4 and 275 mosM. To elicit action potentials, whole-cell current-clamp recordings from both GFP$^+$ and GFP$^-$ cells were performed using the Axopatch amplifier (model 200A; Axon Instruments). From a resting potential of −60 mV, a series of current steps (step size = 10–30 pA; step duration = 300 ms), was applied to depolarize the cell membrane.

After the recordings, the coverslips were immediately fixed with 4% PFA as described in the previous section. To identify cells from which electrophysiological recordings were obtained, biocytin staining or rhodamine$_{600}$ (XRITC) Avidin D fluorescence detection (Vector Laboratories) was used in combination with anti-NeuN antibody (see Immunocytochemistry).

Slice electrophysiological recordings were obtained from P3–P12 CNP-GFP mice. In brief, mice were killed after NIH Animal Welfare Guidelines and 300 μm hippocampal sagittal sections were obtained. After a 1-h recovery period, slices were transferred to a recording chamber and perfused with extracellular solution as described in Online supplemental material. Weakly CNP-GFP$^+$ cells (visualized as described in the legend to Fig. 6 and in Yuan et al., 2002) were identified in the subgranular layer or hilar region of the dentate gyrus and also in CA1/CA3 pyramidal layers, and whole-cell current-clamp was used to investigate the ability of these cells to elicit action potentials. All parameters were as described above for the FACS®-cultured cells, except that the intracellular solution contained 2

mg/ml dextran-conjugated tetramethylrhodamine (Molecular Probes, Inc.) instead of biocytin. This allowed for the immediate visualization of the recorded cells under a fluorescence microscope.

For the recording of spontaneous synaptic currents, CNP-GFP$^+$ cells displaying weak GFP fluorescence in hilar region of the dentate gyrus and CA3 regions were voltage clamped at −60 mV and continuous traces were obtained. Extracellular solution was as described in Online supplemental material, and intracellular solution comprised of (mM): $CsMeSO_4$ 135, NaCl 8, MgATP 4, NaGTP 0.3, Hepes 10, and EGTA 0.6.

Online supplemental material

Fig. S1 illustrates the correlation between loss of CNP-GFP expression and morphological differentiation of GFAP$^+$ astrocytes derived from CNP-GFP$^+$ progenitor cells. Fig. S2 provides evidence that CNP-GFP$^+$ cells derived from transgenic line A2 have similar multipotent properties. Fig. S3 demonstrates that CNP protein is only expressed in mature oligodendrocytes and cannot be detected in GAD67$^+$ hippocampal neurons, which maintain a low level of CNP gene transcription, as detected by GFP fluorescence. Fig. S4 shows subregional differences in the anatomical distribution of NeuN$^+$/CNP-GFP$^+$ cells in the postnatal hippocampus. Online supplemental material available at http://www.jcb.org/cgi/content/full/jcb.200210110/DC1.

We are particularly grateful to Brian Weinberg (National Institute of Child Health and Human Development, NIH, Bethesda, MD) and Robyn Rufner (George Washington University School of Medicine, Washington, DC) for their valuable help in acquisition of confocal images. We thank our colleagues Jeff Mason and James Goldman (Columbia University, New York, NY) for sharing their unpublished observations and for valuable discussion. We thank Douglas Fields, Beth Stevens, and Chris J. McBain for discussion. We thank Regina Armstrong, Li-Jin Chew, Douglas Fields, Chris McBain, Sergio Schinelli, and Beth Stevens for their critical comments on the manuscript.

This work was partially supported by the NICHD intramural program, by P30HD40677, and by the Wadsworth Foundation. S. Belachew was supported by the Fonds National de la Recherche Scientifique (Belgium), and by NICHD. R. Chittajallu was supported by a Wellcome Trust Fellowship. Adan Aguirre was supported by a pre-doctoral fellowship from Consejo Nacional de Ciencia y Tecnologia and from the William A. Haseltine Postdoctoral Fellowship in Neuroscience and Genetics.

Submitted: 18 October 2002
Revised: 24 February 2003
Accepted: 24 February 2003

References

Altman, J., and G.D. Das. 1965. Autoradiographic and histological evidence of postnatal hippocampal neurogenesis in rats. *J. Comp. Neurol.* 124:319–335.

Alvarez-Buylla, A., and S. Temple. 1998. Stem cells in the developing and adult nervous system. *J. Neurobiol.* 36:105–110.

Alvarez-Buylla, A., J.M. Garcia-Verdugo, and A.D. Tramontin. 2001. A unified hypothesis on the lineage of neural stem cells. *Nat. Rev. Neurosci.* 2:287–293.

Bansal, R., and S.E. Pfeiffer. 1997a. FGF-2 converts mature oligodendrocytes to a novel phenotype. *J. Neurosci. Res.* 50:215–228.

Bansal, R., and S.E. Pfeiffer. 1997b. Regulation of oligodendrocyte differentiation by fibroblast growth factors. *Adv. Exp. Med. Biol.* 429:69–77.

Belachew, S., X. Yuan, and V. Gallo. 2001. Unraveling oligodendrocyte origin and function by cell-specific transgenesis. *Dev. Neurosci.* 23:287–298.

Bergles, D.E., J.D. Roberts, P. Somogyi, and C.E. Jahr. 2000. Glutamatergic synapses on oligodendrocyte precursor cells in the hippocampus. *Nature.* 405: 187–191.

Cameron, H.A., and R.D. McKay. 2001. Adult neurogenesis produces a large pool of new granule cells in the dentate gyrus. *J. Comp. Neurol.* 435:406–417.

Capela, A., and S. Temple. 2002. LeX/ssea-1 is expressed by adult mouse CNS stem cells, identifying them as nonependymal. *Neuron.* 35:865–875.

Chiasson, B.J., V. Tropepe, C.M. Morshead, and D. van der Kooy. 1999. Adult mammalian forebrain ependymal and subependymal cells demonstrate proliferative potential, but only subependymal cells have neural stem cell characteristics. *J. Neurosci.* 19:4462–4471.

Dawson, M.R., J.M. Levine, and R. Reynolds. 2000. NG2-expressing cells in the central nervous system: are they oligodendroglial progenitors? *J. Neurosci. Res.* 61:471–479.

Doetsch, F., I. Caille, D.A. Lim, J.M. Garcia-Verdugo, and A. Alvarez-Buylla. 1999. Subventricular zone astrocytes are neural stem cells in the adult mammalian brain. *Cell.* 97:703–716.

Ffrench-Constant, C., and M.C. Raff. 1986. Proliferating bipotential glial progenitor cells in adult rat optic nerve. *Nature.* 319:499–502.

Fuss, B., B. Mallon, T. Phan, C. Ohlemeyer, F. Kirchhoff, A. Nishiyama, and W.B. Macklin. 2000. Purification and analysis of in vivo-differentiated oligodendrocytes expressing the green fluorescent protein. *Dev. Biol.* 218:259–274.

Gage, F.H. 2000. Mammalian neural stem cells. *Science.* 287:1433–1438.

Gravel, M., A. Di Polo, P.B. Valera, and P.E. Braun. 1998. Four-kilobase sequence of the mouse CNP gene directs spatial and temporal expression of lacZ in transgenic mice. *J. Neurosci. Res.* 53:393–404.

He, W., C. Ingraham, L. Rising, S. Goderie, and S. Temple. 2001. Multipotent stem cells from the mouse basal forebrain contribute GABAergic neurons and oligodendrocytes to the cerebral cortex during embryogenesis. *J. Neurosci.* 21:8854–8862.

Johansson, C.B., S. Momma, D.L. Clarke, M. Risling, U. Lendahl, and J. Frisen. 1999. Identification of a neural stem cell in the adult mammalian central nervous system. *Cell.* 96:25–34.

Johe, K.K., T.G. Hazel, T. Muller, M.M. Dugich-Djordjevic, and R.D. McKay. 1996. Single factors direct the differentiation of stem cells from the fetal and adult central nervous system. *Genes Dev.* 10:3129–3140.

Kaplan, M.S., and J.W. Hinds. 1977. Neurogenesis in the adult rat: electron microscopic analysis of light radioautographs. *Science.* 197:1092–1094.

Kondo, T., and M.C. Raff. 2000. Oligodendrocyte precursor cells reprogrammed to become multipotential CNS stem cells. *Science.* 289:1754–1757.

Kuhn, H.G., H. Dickinson-Anson, and F.H. Gage. 1996. Neurogenesis in the dentate gyrus of the adult rat: age-related decrease of neuronal progenitor proliferation. *J. Neurosci.* 16:2027–2033.

Laywell, E.D., P. Rakic, V.G. Kukekov, E.C. Holland, and D.A. Steindler. 2000. Identification of a multipotent astrocytic stem cell in the immature and adult mouse brain. *Proc. Natl. Acad. Sci. USA.* 97:13883–13888.

Lendahl, U., L.B. Zimmerman, and R.D. McKay. 1990. CNS stem cells express a new class of intermediate filament protein. *Cell.* 60:585–595.

Levine, J.M., R. Reynolds, and J.W. Fawcett. 2001. The oligodendrocyte precursor cell in health and disease. *Trends Neurosci.* 24:39–47.

Liu, S., J. Wang, D. Zhu, Y. Fu, K. Lukowiak, and Y. Lu. 2003. Generation of functional inhibitory neurons in the adult rat hippocampus. *J. Neurosci.* 23: 732–736.

Malatesta, P., E. Hartfuss, and M. Gotz. 2000. Isolation of radial glial cells by fluorescent-activated cell sorting reveals a neuronal lineage. *Development.* 127: 5253–5263.

Mallon, B.S., H.E. Shick, G.J. Kidd, and W.B. Macklin. 2002. Proteolipid promoter activity distinguishes two populations of NG2-positive cells throughout neonatal cortical development. *J. Neurosci.* 22:876–885.

Minturn, J.E., D.H. Geschwind, H.J. Fryer, and S. Hockfield. 1995a. Early postmitotic neurons transiently express TOAD-64, a neural specific protein. *J. Comp. Neurol.* 355:369–379.

Minturn, J.E., H.J. Fryer, D.H. Geschwind, and S. Hockfield. 1995b. TOAD-64, a gene expressed early in neuronal differentiation in the rat, is related to unc-33, a *C. elegans* gene involved in axon outgrowth. *J. Neurosci.* 15:6757–6766.

Noctor, S.C., A.C. Flint, T.A. Weissman, R.S. Dammerman, and A.R. Kriegstein. 2001. Neurons derived from radial glial cells establish radial units in neocortex. *Nature.* 409:714–720.

Reynolds, B.A., and S. Weiss. 1992. Generation of neurons and astrocytes from isolated cells of the adult mammalian central nervous system. *Science.* 255: 1707–1710.

Seki, T. 2002. Expression patterns of immature neuronal markers PSA-NCAM, CRMP-4 and NeuroD in the hippocampus of young adult and aged rodents. *J. Neurosci. Res.* 70:327–334.

Seri, B., J.M. Garcia-Verdugo, B.S. McEwen, and A. Alvarez-Buylla. 2001. Astrocytes give rise to new neurons in the adult mammalian hippocampus. *J. Neurosci.* 21:7153–7160.

Song, H., C.F. Stevens, and F.H. Gage. 2002a. Astroglia induce neurogenesis from adult neural stem cells. *Nature.* 417:39–44.

Song, H., C.F. Stevens, and F.H. Gage. 2002b. Neural stem cells from adult hippocampus develop essential properties of functional CNS neurons. *Nat. Neurosci.* 5:438–445.

Spassky, N., C. Goujet-Zalc, E. Parmantier, C. Olivier, S. Martinez, A. Ivanova, K. Ikenaka, W. Macklin, I. Cerruti, B. Zalc, and J.L. Thomas. 1998. Multiple restricted origin of oligodendrocytes. *J. Neurosci.* 18:8331–8343.

Stallcup, W.B., and L. Beasley. 1987. Bipotential glial precursor cells of the optic

nerve express the NG2 proteoglycan. *J. Neurosci.* 7:2737–2744.

Stone, D.J., J. Walsh, and F.M. Benes. 1999. Localization of cells preferentially expressing GAD(67) with negligible GAD(65) transcripts in the rat hippocampus. A double in situ hybridization study. *Brain Res. Mol. Brain Res.* 71:201–209.

Temple, S., and A. Alvarez-Buylla. 1999. Stem cells in the adult mammalian central nervous system. *Curr. Opin. Neurobiol.* 9:135–141.

van Praag, H., A.F. Schinder, B.R. Christie, N. Toni, T.D. Palmer, and F.H. Gage. 2002. Functional neurogenesis in the adult hippocampus. *Nature.* 415:1030–1034.

Vicario-Abejon, C., C. Collin, P. Tsoulfas, and R.D. McKay. 2000. Hippocampal stem cells differentiate into excitatory and inhibitory neurons. *Eur. J. Neurosci.* 12:677–688.

Wolswijk, G., and M. Noble. 1989. Identification of an adult-specific glial progenitor cell. *Development.* 105:387–400.

Yuan, X., A.M. Eisen, C.J. McBain, and V. Gallo. 1998. A role for glutamate and its receptors in the regulation of oligodendrocyte development in cerebellar tissue slices. *Development.* 125:2901–2914.

Yuan, X., R. Chittajallu, S. Belachew, S. Anderson, C.J. McBain, and V. Gallo. 2002. Expression of the green fluorescent protein in the oligodendrocyte lineage: a transgenic mouse for developmental and physiological studies. *J. Neurosci. Res.* 70:529–545.

Yung, S.Y., S. Gokhan, J. Jurcsak, A.E. Molero, J.J. Abrajano, and M.F. Mehler. 2002. Differential modulation of BMP signaling promotes the elaboration of cerebral cortical GABAergic neurons or oligodendrocytes from a common sonic hedgehog-responsive ventral forebrain progenitor species. *Proc. Natl. Acad. Sci. USA.* 99:16273–16278.